NPS-61-[redacted]Nb 75121

NAVAL POSTGRADUATE SCHOOL

Monterey, California

LASER EFFECTS HANDBOOK

3 LASER ABSORPTION WAVE PHENOMENA

Don E. Harrison, Jr.
John R. Neighbours, Editor

DECEMBER 1975

Approved for Public Release

NAVAL POSTGRADUATE SCHOOL
Monterey, California

Rear Admiral Isham Linder
Superintendent

Jack R. Borsting
Provost

The work reported herein was supported by the Naval Systems Sea Command. Reproduction of all or part of this report is authorized.

This report was prepared by

UNCLASSIFIED

SECURITY CLASSIFICATION OF THIS PAGE *(When Data Entered)*

REPORT DOCUMENTATION PAGE

READ INSTRUCTIONS BEFORE COMPLETING FORM

1. REPORT NUMBER: NPS - 61Nb 75121	2. GOVT ACCESSION NO.
3. RECIPIENT'S CATALOG NUMBER	
4. TITLE *(and Subtitle)*: LASER EFFECTS HANDBOOK 3 LASER ABSORPTION WAVE PHENOMENA	5. TYPE OF REPORT & PERIOD COVERED: Interim Report 1972 - 1974
	6. PERFORMING ORG. REPORT NUMBER
7. AUTHOR(s): Don E. Harrison, Jr. John R. Neighbors, Editor	8. CONTRACT OR GRANT NUMBER(s)
9. PERFORMING ORGANIZATION NAME AND ADDRESS: Naval Postgraduate School Monterey, California 93940	10. PROGRAM ELEMENT, PROJECT, TASK AREA & WORK UNIT NUMBERS: N00024-75-WR-5221
11. CONTROLLING OFFICE NAME AND ADDRESS: Department of the Navy Naval Sea Systems Command Washington, DC 20362	12. REPORT DATE: December 1975
	13. NUMBER OF PAGES: 47
14. MONITORING AGENCY NAME & ADDRESS*(if different from Controlling Office)*	15. SECURITY CLASS. *(of this report)*: UNCLASSIFIED
	15a. DECLASSIFICATION/DOWNGRADING SCHEDULE

16. DISTRIBUTION STATEMENT *(of this Report)*

Approved for public release; distribution unlimited.

17. DISTRIBUTION STATEMENT *(of the abstract entered in Block 20, if different from Report)*

18. SUPPLEMENTARY NOTES

19. KEY WORDS *(Continue on reverse side if necessary and identify by block number)*

Lasers	Laser Irradiation
Plasma	LSA Waves
Plasma Ignition	Material Response

20. ABSTRACT *(Continue on reverse side if necessary and identify by block number)*

Possible plasma ignition mechanisms as a result of laser irradation are listed and individually discussed. Experimental evidence is cited when available. A qualitative discussion of the transition process is given and one demensional laser supported absorbtion waves are discussed.

DD FORM 1 JAN 73 1473 EDITION OF 1 NOV 65 IS OBSOLETE
S/N 0102-014-6601 |

SECURITY CLASSIFICATION OF THIS PAGE *(When Data Entered)*

PREFACE

This is an interim report on an active research field. It contains a comprehensive coverage of those factors which influence LSA ignition, provides a useful introduction to the mathematical treatment of LSA wave propagation and reaches certain conclusions about LSA wave ignition.

During the period between completion of the manuscript and publication of this report, investigation of these problems has continued and thus many of the speculations reported here have since been confirmed.

CONTENTS

LASER ABSORPTION WAVE PHENOMENA

Don E. Harrison, Jr.
Physics and Chemistry Department

1.0 INTRODUCTION AND SYMBOLS

(U) The topics discussed here appear in the literature under a variety of headings. Chief attention will be focused upon Laser Supported Detonation (LSD) waves and Laser Supported Combustion (LSC) waves. It is convenient to group these two phenomena under the more general heading of Laser Supported Absorption (LSA) waves, which includes both surface initiated and gas initiated LSC and LSD waves as well as plasmons or plasmatrons, which describe a related phenomenon, a plasma which does not detach from the target surface. The best available summary of current thinking on these topics is Volume V of the Proceedings of the October 1973 LASER EFFECTS/HARDENING CONFERENCE in Monterey, California[1]. Warning: Understanding has increased, and many individual positions on controversial topics have been modified since its publication!

(U) The introductory article in reference 1 by P. E. Nielsen[2] is a valuable overview of many of the topics discussed here. The entire field of study depends to a large extent upon the initial analysis by Raizer[3], published in 1965. A useful discussion of the relationship between the various phenomena is contained in a report by Nielsen and Canavan[4] which is unpublished.

(U) This article considers a family of effects which appear when laser radiation with irradiance of the order of 10^5 to 10^8 watts/cm^2 is incident upon a solid target in air at pressures above approximately 0.1 atm. Under these conditions a plasma forms at the target surface and then may move back along the laser beam if the irradiance is sufficiently large. If the plasma expansion along the beam is subsonic, the phenomenon is called an LSC wave; if it is supersonic, the wave is an

LSD wave. The general propagation characteristics of the two types of waves have been known for some time, but significant aspects of their propagation and initiation are still under active investigation. For present purposes, initiation has been divided into two steps: ignition in which the first few ions and/or electrons are produced, and transition which carries the initial ionization into a full blown plasma which is propagating as an LSA wave.

(U) LSA ignition occurs at irradiance levels which are two orders of magnitude lower than those normally associated with gas breakdown and spark formation, the gas initiated LSA phenomena. The laser-target interaction is poorly understood; so a large number of ignition mechanisms have been proposed. Hopefully this review can decrease the size of this list of candidates.

(U) Once ignited, the transition to full LSA wave status occurs by well understood physical processes. Unfortunately the details of the transition depend upon the characteristics of the laser (particularly its wavelength) and upon the interaction of a number of competing processes. The role of each process can be identified, but its relative contribution to the transition phenomenon is uncertain. As a result, no detailed theory of transition for a particular target-laser-atmosphere system exists, even though transition times can be estimated with some confidence.

(U) This article surveys the propagation of LSA waves so that the differences between LSC and LSD waves can be clearly established. It also provides background information about hydrodynamics.

1.1 SYMBOLS

The symbols listed here are in the order of their appearance in the article.

λ	wavelength
ρ	density
	subscripts
	m metal
	v vapor
	1 ambient air
	2 shocked air
v	speed of vaporizing surface
G	irradiance
L_m	heat of vaporization of metal
C_m	specific heat of metal
T	temperature
j_+	ion current
j_-	electron current
ϕ_+	positive ion surface work function
ϕ	electron work function
I_s	ionization energy of an atom
ℓ_s	atomic sublimation energy from metal surface
j_o	vaporization current of neutral atoms from a target surface
k	Boltzmann's constant
ν	frequency of radiation
T_c	lifetime of an electron heating cycle
e	electron charge
N_e	electron density

N_p	critical electron density for opaque plasma
P	pressure
V	specific volume, that is, volume per unit mass $V = 1/\rho$
e	specific internal energy
u	fluid flow velocity in LAB system
u*	fluid flow velocity in COM system
h	specific enthalpy
τ	volume element
D	shock front propagation velocity
q	$= G/\rho_2 u_2^*$
j	$= u_2^*\rho_2 = u_1^*\rho_1$
C_p	$(\partial h/\partial T)_p$
C_v	$(\partial e/\partial T)_v$
α	C_p/C_v
c	speed of sound
K	absorption coefficient
β	thermal conductivity

2.0 PLASMA IGNITION

(U) At least ten ignition mechanisms have been proposed since 1971. In some cases the proposal consists of little more than a name, while in others a relatively complete theory has been developed. Many of the ideas were developed through private communications; so it is exceedingly difficult to correctly attribute them to their originators. The situation is further complicated by the intermixing of ignition and transition processes in the presentation of a particular mechanism. Both Nielsen[2] and Walters[6] attempt to give proper credit; so these references should be consulted by the historian.

(U) This review will take another direction. The ignition mechanisms will be grouped by type, and then the common and distinctive features can be more readily identified. The five types are: atom emission, ion emission, electron emission, photon mechanisms and shock wave mechanisms. This organization will facilitate the description of the ignition process.

(U) The experimental fact is that a plasma forms near (within 500 μm) the target surface within a very short time. This time is of the order of 50 nsec for LSD waves and somewhat larger for LSC waves. The plasma contains ions from both the target and from the atmosphere. In all probability it is formed by ions attributable to both sources, but there is some evidence that atmospheric ions appear first in the LSD environment while target ions appear first in the LSC environment. In either event, the transition plasma feeds upon both sources, and the plasma which can be examined spectroscopically contains ions from both. Because of the nature of this review both possibilities will be discussed in some detail; so that the information will be available regardless of the ultimate experimental resolution of the present dilemma. The available experimental conclusions can then be discussed in context.

(U) The ignition of LSA waves is closely related to the more general problem of laser-induced particle emission from surfaces. Many experiments have been performed with ruby lasers (λ = 0.6943 μm → 1.78 eV

photons) which are quite comparable to the Nd-YAG/glass (λ = 1.06 μm → 1.17 eV) and CO_2 (λ = 10.6 μm → 0.117 eV) experiments reported by the LSA specialists. These investigations have been surveyed by Ready[7], whose book should be consulted for further details.

(U) As a general principle, ignition effects rooted in thermal processes should vary little between ruby and CO_2 wavelengths. The thermionic emission of electrons must fall into this group. In contrast, photon sensitive processes such as the photoelectric effect would hardly be comparable because of the difference in photon energy. In the succeeding sections ruby laser results will be included when appropriate.

2.1 IGNITION MECHANISMS

2.11 (U) Atom emission from the target is one plausible source for the plasma if ionization mechanisms are also available. The atoms may be of the target species, from a surface oxide layer (in which case the emitted species may be a molecule, AlO, for example), from surface included material (laid down during polishing and finishing), or from simple 'dirt' which can find its way to the surface in untold number of ways.

(U) There will be a characteristic vaporization temperature for each of the possible species, a specific heat for each, and a latent heat of vaporization for each. Momentum conservation guarantees that the emission process would be thermal, which implies that the vaporization temperature determines the velocity distribution of the emitted atoms. The mean emission speed of the vapor is determined by the conservation of mass and energy and the parameters of the source and emitted material.

(U) As an example, consider emission from a perfectly clean metallic target. Then conservation of mass requires that:

$$\rho_m v_m = \rho_v v_v \ ;$$

here v_m is the speed with which the vaporization surface penetrates the metal, and conservation of energy requires that:

$$v_m = G/(\rho_m[L_m + C_m T_m]).$$

The vaporization speed is difficult to determine, so use a relation proposed by Anisimov, et.al.[8]:

$$v_m = c_m \exp-(L_m/C_m T_m).$$

After some algebra the vapor speed, v_v becomes

$$v_v = AL_m \quad , \tag{1}$$

with

$$A = [2\ell n(\rho_m L_m c_m/G)]^{1/2} .$$

The emission speed is of critical importance because it scales the time available before the atom leaves the laser beam, and hence the time available for the ionization processes.

(U) In a multispecies environment only a fraction of the irradiance, G, say $\alpha_i G$, couples to each species, but otherwise the analysis is the same, and the emission speed scales with the squareroot of the latent heat of vaporization. Actually the problem is even more complicated because surface species will be heated first; so the steady state emission process envisioned here is an idealization.

(U) Ignition mechanisms of this type must be strongly target material sensitive. They will also be sensitive to the target surface condition; so the ignition characteristics might change from pulse to pulse as the laser flux cleaned the surface. This pulse to pulse variation is plausible whether the actual mechanism depend upon an oxide coating, inclusions, or dirt. If the laser pulse rate is not too high an oxidized surface maintained by the atmosphere, again Al is a good example, would have time to reconstitute between pulses.

(U) Because this mechanism depends upon pure heating it would depend strongly upon the laser intensity, but rather weakly upon the laser frequency.

(U) Very high energy neutral particles are also emitted from targets[7]. The energy of CO molecules have been measured by time-of-flight techniques to be 14 eV at 10 MW/cm^2 irradiance and 500 eV at 140 MW/cm^2 from Q-switched ruby lasers. Thermal emission at these energies would require a surface temperature of the order of 10^5 K, which is highly unlikely, because the CO molecule would certainly dissociate at such temperatures. It is possible that the neutral was formed by recombination outside the target after emission, or that these high energy neutrals were formed by charge exchange. These effects have been included here for completeness, but there is only a low probability that these high energy neutral species are directly emitted from the target; so they are not candidates for ignition source.

2.12 (U) Ion emission adds an additional complication to the atom emission discussed above. If the surface temperature is sufficiently high an appreciable fraction of the emitted atoms will be ionized. If the emitted particles are singly ionized the Richardson-Smith equation applies, and the ion current is given by:

$$j_+ = A_+ T^2 \exp(-\phi_+/kT)$$

where A_+ is a constant, T is the absolute temperature, and ϕ_+ is the positive ion work function. ϕ_+ is essentially unknown, but it can be estimated by the argument that the energy required to remove the singly charged ion, ϕ_+, plus the energy required to remove a single electron, ϕ, should equal the energy required to remove a neutral atom, ℓ_s, plus the ionization energy of the neutral atom, I_a. This argument applied to Al gives $\phi_+(Al) = 5.3$ eV, and to Cu gives $\phi_+(Cu) = 7.25$ eV. For comparison, $\phi(Al) = 3.6$ eV and $\phi(Cu) = 4.4$ eV. Thus the positive ion emission will be considerably smaller than the electron emission at the same temperature. The Richardson-Smith equation is only an approximation; so it should be used with caution.

(U) Even less reliable is the Saha-Langmuir equation which is derived under equilibrium assumption, but is often applied to determine the fraction of the particle current which is ionized by the laser beam.

In particular, target surface temperatures obtained in this way are highly suspect. The Saha-Langmuir equation predicts that the fraction ionized takes the form

$$j_+/j_o \sim \exp[(\phi - I_a)/kT].$$

As the ionization potential is generally larger than the work function the degree of ionization must increase rapidly with temperature. From Q-switched ruby laser data at 6 MW/cm^2 the duration of the emitted ion pulse is $\sim$ 100 nsec, which is of the order of magnitude required for the prompt ignition of LSD waves.

(U) Time-of-flight energy measurements on the ions emitted by Q-switched ruby laser experiments give energies of the order of 1000 eV. As surface temperatures never approach such values plasma effects must be influencing the ion emission process. Multiphoton effects of this magnitude are considered to be totally out of the question.

(U) Ion emission from oxide layers and/or 'dirt' is certainly possible, but is too dependent upon the details of a particular targets condition for general discussion. High energy molecules containing atoms from surface species, particularly oxides, are readily detected as molecular ions, but the ionization may have occurred after emission.

(U) The preceding discussion makes use of temperatures, which implies that the materials are at least approximately in thermal equilibrium. This assumption may not be justified, even though no non-equilibrium effects have ever been positively identified. In particular, in the presence of the electron emission processes discussed in the next section, strong electrostatic forces must be applied to ions near the target surface, and non-equilibrium emission processes become possible. When many electrons have been stripped from the surface region, heavy positively charged ions remain; so that a large fraction of the target atoms emitted could be ionized. Charge conservation at the target surface becomes a major consideration.

(U) In summary, it is possible to visualize processes by which the

target could emit a significant number of ions in a short period of time, but the processes depend upon detailed considerations of particular materials and surface conditions which defy analysis at the present time.

2.13 (U) Electron emission processes are the most likely ignition mechanism for LSD waves. Thermionic emission is known to be present, and if the laser pulse shape is known the shape of the electron pulse can be calculated from the Richardson-Dushman equation. This equation can be derived from either thermodynamic[9] or kinetic[10] theory arguments. The usual form is

$$j_- = A_- T^2 \exp(-\phi/kT),$$

where j_- is the electron density, ϕ the electron work function of the target surface, and A_- is a universal constant ($A_- = 60.2$ A $cm^{-2}deg^{-2}$) for many metals. Ready[7] shows that the Richardson-Dushman equation is a reasonable description of the electron emission from normal laser pulses, and that thermionic emission of the order of mA/cm^2 is readily produced within 50 nsec by Q-switched ruby lasers[11]. These measurements were performed at 10^{-8} torr. At higher pressures where absorbed gases become more prevalent the electron emission rises, which indicates that electron emission can also occur from surface materials.

(U) Thermionic emission is also influenced by surface morphology. If the surface contains pits, protrusions, or inclusions, the local temperature may be much higher than would be predicted from the laser flux and thermal properties of the bulk target material. The temperature at the tip of a protrusion will be significantly higher than that of the surrounding material because the tip is unable to dissipate heat to the bulk of the material so rapidly as a planar surface can.

(U) Surface atoms, whether oxide layers, or 'dirt', disrupt the lattice periodicity of the target, and affect the work function of the surface. At $\phi = 5$ eV, a one percent reduction of the work function causes an 80 percent increase in j_- at 1000 °K. A few surface atoms produce noticable effects, a monolayer of coverage completely changes the work function. Because all materials emit thermionically, at high

irradiance, target material effects will appear primarily in the time dependence of j_-, that is in the shape of the electron pulse ignited by the laser pulse.

(U) Field enhanced emission from cold targets is a very prompt mechanism, and therefore is attractive as a LSD wave ignition process. Musal has explored this possibility[12] from the viewpoint of the Fowler and Nordheim analysis[13] which is also discussed in the Dushman article cited above[9]. Musal has done the calculations for laser irradiances in the range from 50 to 500 MW/cm^2 and finds that the electric field strength is approximately two orders of magnitude too small for the effect to be significant for electron emission from a plane surface. However, when surface features are included in the analysis the field strength is greatly enhanced, and the mechanism becomes feasible. Photon assisted field emission has recently been discussed by Caroli, et.al.[14].

(U) Schottky emission, thermionic emission in the presence of an external electric field, has also been extensively studied. This is a quantum mechanical barrier penetration process in which the work function is field dependent[15]. The analysis shows that the work function will be reduced, but that otherwise the process is similar to thermionic emission[16]. Fields of the order of 10^5 volts/cm cause a very small lowering of ϕ. The power of T in the pre-exponential factor of the Richardson-Dushman equation is difficult to determine experimentally, particularly in the field-enhanced environment. The factor may well be T^3 rather than Richardson's T^2 in the LSA experiments, because there is considerable experimental simularity between the ignition experiments and the 'complete photo-electric effect'[16].

(U) Multiphoton emission processes can produce significant electron current density from ruby and Nd doped glass laser photons. The mechanism is hardly feasible from the low energy photons of the CO_2 laser. The mechanism has been included here because it gives the earliest response of any of the mechanisms proposed. Multiphoton processes become particularly significant for pico-second laser pulses when the irradiance is small so that there is little temperature rise in the target. Thermionic

emission decreases exponentially as the irradiance decreases, while a two-photon emission process decreases as the square of the irradiance; so at some level the two effects must be equal, but this normally occurs at irradiance levels well below those required to initiate LSA waves.

2.14 (U) Photon emission mechanisms are poor candidates for LSA ignition. The two immediate possibilities are reflected photons from the laser pulse and photons generated in the target. The reflected photons are not sufficiently energetic to cause appreciable ionization, but their effect can be included under the field emission heading because they do increase the effective electric field[12]. Photons from the target could be either thermally emitted by the hot target surface, or emitted as the result of a multiphoton atomic process which occurs at the surface.

(U) Although sufficient energy is available to melt the target surface and/or vaporize it under some conditions, the temperatures reached are realtively low, and only low energy photons would be produced. Such photons probably exist, but they can have little effect upon the transition from ignition to plasma; so it seems unlikely that they can be major contributors to the LSA initiation process.

(U) Multiphoton atomic process could make some contribution for ruby laser or Nd/glass illumination, but not for CO_2 illumination because the photon energy is so small that 10-20 photon process would be required. There is not experimental evidence that photon processes contribute significantly to LSA ignition.

2.15 (U) Thermomechanical response of the target to the laser pulse has been proposed as an ignition mechanism by Steverding[12]. In this model, rapid heating in a shallow region near the target surface produces a compression stress wave which propagates to the target surface as a shock wave. The shock wave produces spallation at the surface. The emission velocity is the shock velocity, and the emitted material is a plasma because the shock wave has both vaporized and ionized the target material.

(U) As envisioned, the target is heated for a relatively long time (20 μsec) and the laser energy is deposited in a very shallow region (10^{-4}cm = 1 μm). This last assumption requires a depth of penetration, a skin depth, of approximately λ/10 for the CO_2 laser pulse. A region of this depth is consistent with the calculation of Ready[11], for the first 50 nsec of the pulse, but thermal conduction increases the depth by an order of magnitude within the first 200 nsec. This mechanism appears to be too slow for LSD ignition, but it may be feasible for LSC ignition.

2.2 IGNITION EXPERIMENTS

(U) Experimental study of LSA wave ignition processes cannot presently be separated from effects attributable to transition processes, but certain mechanisms can be ruled out by more general properties of LSA waves. Here some of the experimental properties of LSC and LSD waves are summarized and interpreted in the light of the various proposed mechanisms. Ignition of LSC waves differs sufficiently from LSD ignition that they are considered separately. Much more experimental effort has been devoted to LSD waves, see the reports by Hall, et.al.[18]; Walters[6]; and Musal[12]; so the ignition properties are more completely determined. Pertinent LSC results have been reported by Fowler and Smith[19]; Conrad, Mangum, and Gurley[20]; and Thomas[21] who has used computer simulations to good effect.

(U) This survey will not discuss LSB (Laser Supported Blast) effects in detail. These spherical shock waves occur in conjunction with LSC and LSD waves, but are not supported by the laser. Hall, et.al.[18] have pictures and a discussion. Target vapor 'microjets' are also observed[18], which move normal to the target surface; so if the target is inclined with respect to the laser beam direction they are easily distinguished from LSC and LSD waves. Microjets 'ignite' much more slowly than LSD waves, but on a time scale comparable to LSC wave ignition times.

(U) Vacuum ignition of Al targets by nsec duration Nd-glass laser pulses of irradiance $G_p \simeq 10^{10}$ W/cm^2 have been studied in some detail by Brooks[22]. Note that the targets were held in a relatively good vacuum ($\sim 10^{-5}$ torr), and the irradiance is three orders of magnitude greater than that associated with LSD wave ignition, but that the total energy absorbed by the target is comparable to that reported in the LSC and LSD experiments.

2.21 (U) Laser supported combustion wave ignition occurs in the irradiance range $2 \times 10^5 \leq G_p \leq 6 \times 10^6$ W/cm^2. Hall, et.al.[18] has observed LSC waves in the short pulse (~ 20 μsec) CO_2 laser system in which their LSD experiments were performed. They have not made extensive studies of LSC wave initiation or propagation. The detailed information currently available comes from the cw CO_2 laser studies of Fowler and Smith[19], and the long pulse (~ 1 sec) CO_2 laser studies of Conrad, Mangum, and Gurley[20].

(U) When compared with the LSD wave experiments the single most outstanding difference is the relatively long initiation time of the LSC waves. If the initiation time is defined as the time until the LSA becomes detectable, both ignition and transition must occur during the initiation period. This time is of the order of 200 μsec for LSC waves, which must be compared with LSD initiation times of the order of 50 nsec. LSC is very much slower, more than three orders of magnitude, so the ignition processes must be very different. On the assumption of a linear rise and that G_p occurs after 200 μsec, the target surface absorbs ~ 100 J/cm^2 from a $G_p = 10^6$ W/cm^2 laser before initiation. With this time span and this much energy available, even the slower ignition mechanism, such as atom and ion emission, are feasible. When comparable laser irradiations are applied to targets in vacuum chambers, where the pressure is of the order of 0.1 atm, plasma microjet phenomena are observed. Thus target vaporization with consequent emission of atoms and/or ions seems to be an observable characteristic of this irradiance region. Thomas[21] has done computer simulations based upon vaporization ignition which compare very favorable with the MSNW experiments[23].

(U) In summary, target vaporization mechanisms appear to be sufficiently to explain the existing information about LSC ignition, but the necessity of these mechanisms has not been established. The faster electron emission mechanisms certainly have the opportunity to function, but the irradiance may be insufficient to initiate a surface plasma. Sufficient energy has been dumped into the surface that thermionic emission must occur but the field strength contribution from the irradiance minimized the Schottky emission contribution. Thus there is indirect evidence that the Schottky mechanism is an important contributor to LSD ignition.

2.22 (U) Laser supported detonation wave ignition occurs in the irradiance range $2 \times 10^7 \leq G_p \leq 5 \times 10^7$ W/cm^2. Most of the pertinent experimental information on LSD ignition has been obtained by Hall, et.al.[18], and by Walters[6] who has also done a detailed integration of the experimental evidence applicable to the ignition problem available at the time of his review.

(U) LSD waves ignite very promptly; the initation time is of the order of 50 nsec. Quite independent of the target material the initiation occurs after the target has absorbed approximately 1.7 J/cm^2 of energy. This value was obtained by Walters[6] who integrated his experimental laser pulse shape out to the initiation time. This is insufficient energy for uniform surface vaporization to occur, but it is consistent with either a thermionic or Schottky emission mechanism. At this irradiance the rms electric field strength is insufficient to produce field emission from a plane surface; so the Schottky mechanism is indicated.

(U) Walter's careful studies of the ignition process indicate that LSD waves ignite from 'numerous individual luminosity sites'. The wave front forms when the emission from these sites combine in front of the target surface. He has done careful scanning electron microscope (SEM) studies of target surface, and has compared the appearance of an individual surface feature before and after LSD wave ignition. The pictures are in ref. 6. A feature identified before the laser pulse is immediately recognizable after the pulse. The SEM scans an area 50 by 250 μm at a

2000X magnification. Although absolute correlation between surface features and luminosity sites has not been accomplished the evidence that features cause luminosity sites is very strong.

(U) The laser pulse does cause surface damage, and it does change the surface features, but there is no gross change in any feature which could be associated with significant vaporization of its surface. When all of the data are taken together electron emission from surface features appears to be the most likely ignition mechanism. The ignition may be thermionic, field emission as proposed and discussed by Musal[12], or a Schottky effect combination of the two at the surface feature. Vaporization from surface features can certainly occur, but it must be a second order effect because the features exhibit so little damage, and electron emission is dominant.

(U) Tables I and II from Hall, et.al.[18] give LSD ignition thresholds as measured by image convertor photographs and by measurement of a reflected signal. The agreement is relatively good when the lack of uniformity of the surfaces is considered.

(U) Table III is Walter's summary[6] of the relative importance of the various LSD ignition models which have been proposed.

TABLE I

THRESHOLDS FOR IGNITION OF LASER-SUPPORTED ABSORPTION WAVES USING A 28 CM FOCAL LENGTH LENS AND USING A NEW SPECIMEN FOR EACH TEST AT ONE ATMOSPHERE. THRESHOLD DETERMINED BY IMAGE CONVERTER PHOTOGRAPHS OF LUMINOSITY.

Material	E_T (joules/cm^2)	q_{max} (watts/cm^2)
Copper Foil	266	3.83×10^7
Lucite	258	3.72×10^7
Polished Tungsten	229	3.30×10^7
Copper Plate	192	2.8×10^7
Tungsten Plate (unpolished)	186	2.68×10^7
Aluminum (7075 alloy)	176	2.53×10^7
Aluminum Foil	160	2.30×10^7
Tantalum	128	1.84×10^7
Carbon	88	1.27×10^7
Aluminum Black (very heavily anodized Al)	87	1.25×10^7
Lead Foil (polished)	64	$.92 \times 10^7$
Lead Plate (unpolished)	43	$.62 \times 10^7$

TABLE II

THRESHOLDS FOR IGNITION OF LASER-SUPPORTED ABSORPTION WAVES USING A 28 CM FOCAL LENGTH LENS AND USING A NEW SPECIMEN FOR EACH TEST AT ONE ATMOSPHERE THRESHOLD DETERMINED BY MEASURING REFLECTED SIGNAL.

Material	E_T(joules/cm^2)	q_{max}(watts/cm^2)
Fused Silica	310	4.5×10^7
Lucite	310	4.5×10^7
Lexan (polycarbonate)	280	4.0×10^7
H_2O	220	3.2×10^7
Teflon	195	2.8×10^7
Copper	191	2.75×10^7
Painted Aluminum (.001 cm gloss black lacquer)	173	2.5×10^7
Titanium	160	2.3×10^7
Fiberglass Epoxy	158	2.3×10^7
Cork	144	2.1×10^7
Nickel	137	1.97×10^7
Tungsten	124	1.79×10^7
Soda Glass	106	1.52×10^7
Painted Aluminum (.004 cm red enamel)	85	1.22×10^7
Aluminum Foil	84	1.2×10^7
Aluminum 7075 Plate	75	1.08×10^7
Lead	68	$.98 \times 10^7$
Alumina	59	$.85 \times 10^7$
Painted Aluminum (.004 cm flat black lacquer)	42	$.60 \times 10^7$

TABLE III

ASSESSMENT OF THE ROLE OF VARIOUS MECHANISMS IN LSD WAVE INITIATION ON PRACTICAL ALUMINUM SURFACES

Mechanism	Role	Experimental Basis
(1) Uniform target vaporization	None	SEM, photography, breakdown time
(2) Oxide vapor absorption	Minor	Oxide-free surface initiation
(3) Chemical reaction	Unknown*	
(4) Thermionic emission	Major	Target emission, breakdown time, pressure dependence of threshold
(5) Planar reflection	No independent role for $G_p<5X10^8$	Clean-air breakdown
(6) Local target heating	Major	SEM, photography
(7) Contaminant and gas desorption	Variable	Contaminant-free surface
(8) Field emission	Minor for $GP<3X10^8$	SEM, bent sample, breakdown time
(9) Shock heating of the air	Unknown*	
(10) Nonequilibrium ionization of vapor	Unknown*	
(11) Defect-enhanced fields	Minor for $G_p<3X10^8$	Breakdown time

* Spectroscopy now underway should provide assessment.

2.23 (U) Plasma emission experiments are discussed in this section. Although there is no direct evidence that these results bear directly upon the LSA ignition problem the similarities are sufficiently striking that the connection may ultimately be made.

(U) The experiments, performed by Brooks[22], used a Q switched Nd-glass laser with energy between 2.5 and 12 joules. The pulse duration was 25 nsec, and the focal spot size was ~ 0.018 cm^2; so the irradiance was $1.4 \times 10^9 \leq G_p \leq 5.7 \times 10^9$ W/cm^2. Note that the total energy fluence absorbed by the target (140-700 J/cm^2) is comparable to that reported in the LSC and LSD experiments.

(U) The laser pulse produces a burst of plasma from an Al target. Careful analysis of the plasma by probes determined that it consists of 3 components which are described in Table IV.

TABLE IV

Component	Emission Time	Speed	Density
first early	3 nsec	1.1×10^6 m/sec	2.5×10^{12}/cm^3
second early	12 nsec	5.9×10^5 m/sec	2.5×10^{12}/cm^3
main	0-10 nsec	1.1×10^5 m/sec	10^{14}/cm^3

(U) A very prompt (< 1 nsec) electromagnetic pulse was also detected. Experimental studies confirmed that its wavelength is less than 0.4 μ; so it was not a reflection of the incident laser pulse.

(U) An applied magnetic field has little effect on the early pulses; so they cannot be purely electronic in nature. Heavy ions must be present; hence the term "plasma pulse" seems appropriate. The main pulse is delayed by the applied magnetic field (B = 950 gauss). The delay is consistent with an interpretation which finds the plasma front relatively rich in electrons while the main body is richer in ions[24-26].

(U) The early plasma pulse(s) have been mapped with probes. Figure 1 shows the plasma extent after 20 nsec. The two early pulses have not

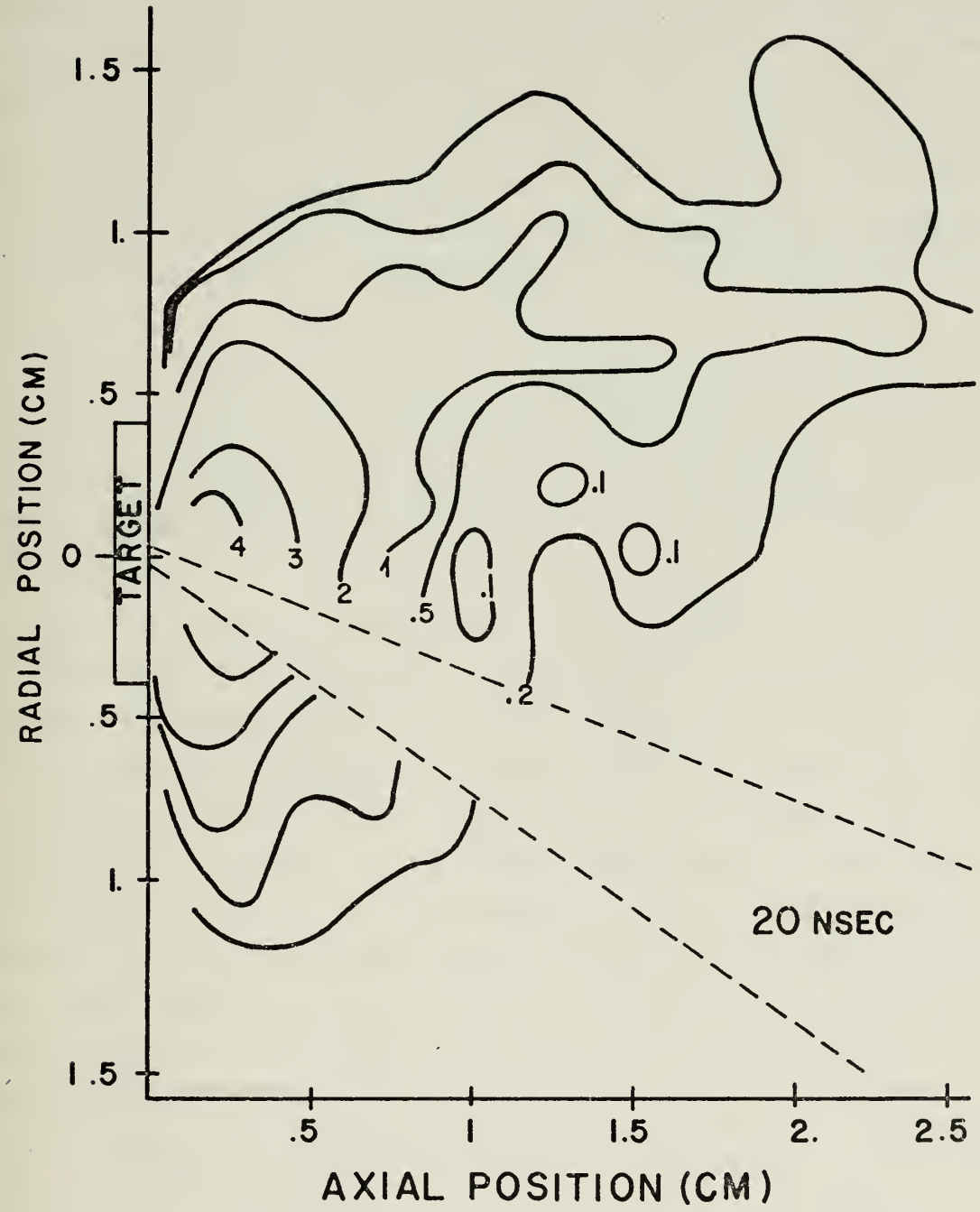

Fig. 1 Relative density contours for a laser produced plasma 20 nsec after ignition. See text for details

separated at this time. Note that the plasma is asymmetrical and appears to be expanding along the specular reflection direction. The plasma has expanded out to the beam spot, and is now eroding the entire target surface. Experiments performed on large area targets show that after 50 shots the naked eye visual erosion region has an area of ~ 1 cm^2 when the focal area is 0.018 cm^2. Microscopic analysis of a larger region has not been carried out, Figure 1 suggests that the plasma extends beyond this range.

(U) The plasma contours after 160 nsec are shown in Figure 2. Note that the two early pulses have now separated from the main plasma (one is still visible on the right hand side of the figure). The plasma emission is now symmetrical, and the main pulse is moving normal to the target surface.

(U) The situation after 800 nsec is shown in Figure 3. Note in particular that the plasma is still attached to the target; so that it is still feeding upon the target by sputtering.

(U) This material has been included because it demonstrates the target material behavior when it expands into an atmosphere of comparable density ($n \simeq 10^{13}/cm^3$). At a standard atmosphere the plasma would interact much more strongly with the background gas; so the development must be much more complicated than illustrated here. Still certain similarities should remain. The prompt emission from the target should not be background pressure sensitive. The electron-rich front surface of the main plasma burst is a target phenomenon which should carry over. Note that it supports the idea that the initial emission must be electronic with ions following closely. This effect will be discussed in greater detail below. Even though the laser pulse has been extinguished for almost 0.8 μsec in Figure 3 the plasma is still feeding on the target as it expands away from the surface. There is strong evidence that the radial expansion of the plasma is constrained by a self-induced magnetic field[22-27]. This would help to explain the long time of contact between the plasma and the target surface.

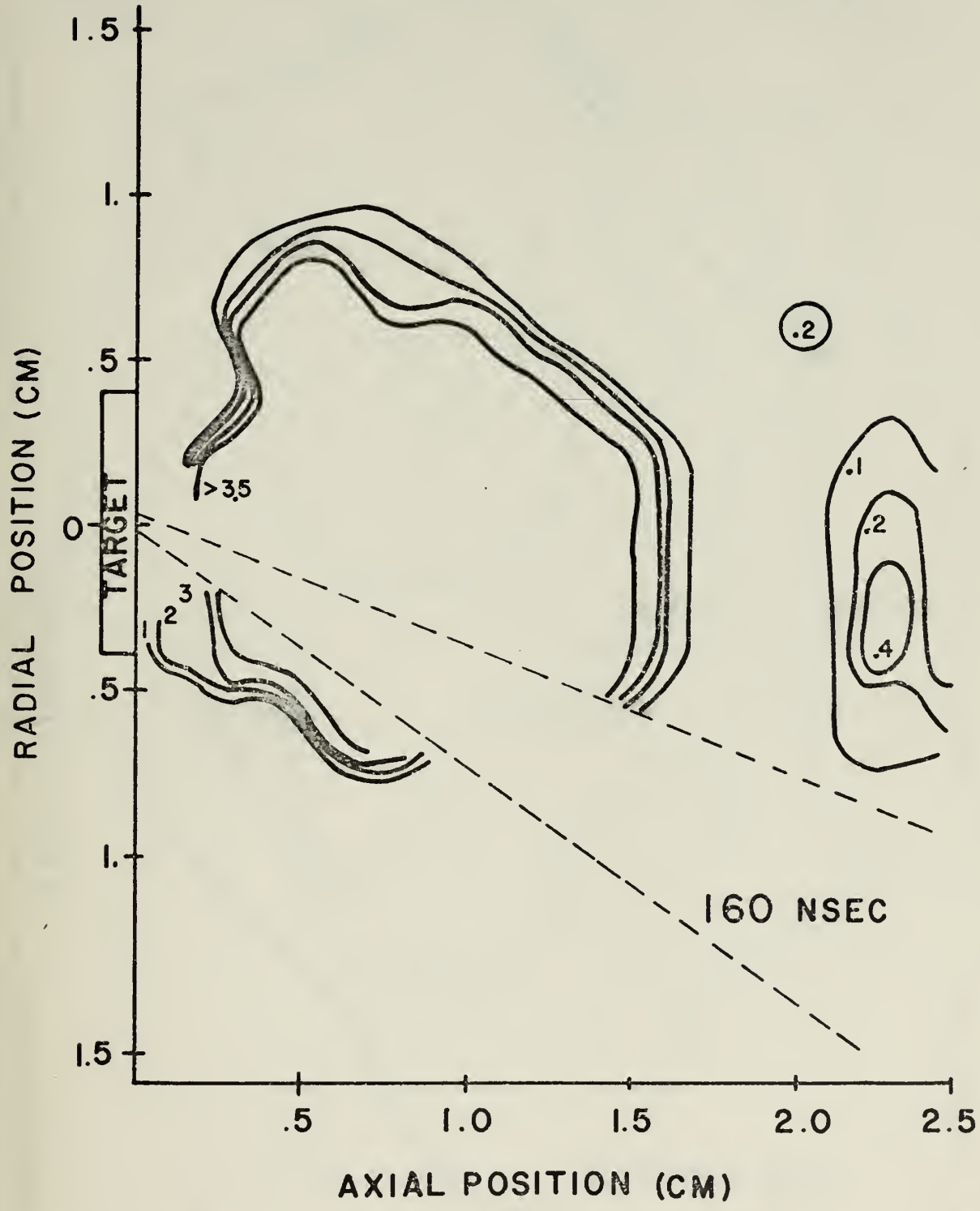

Fig. 2 Relative density contours for a laser produced plasma 160 nsec after ignition.

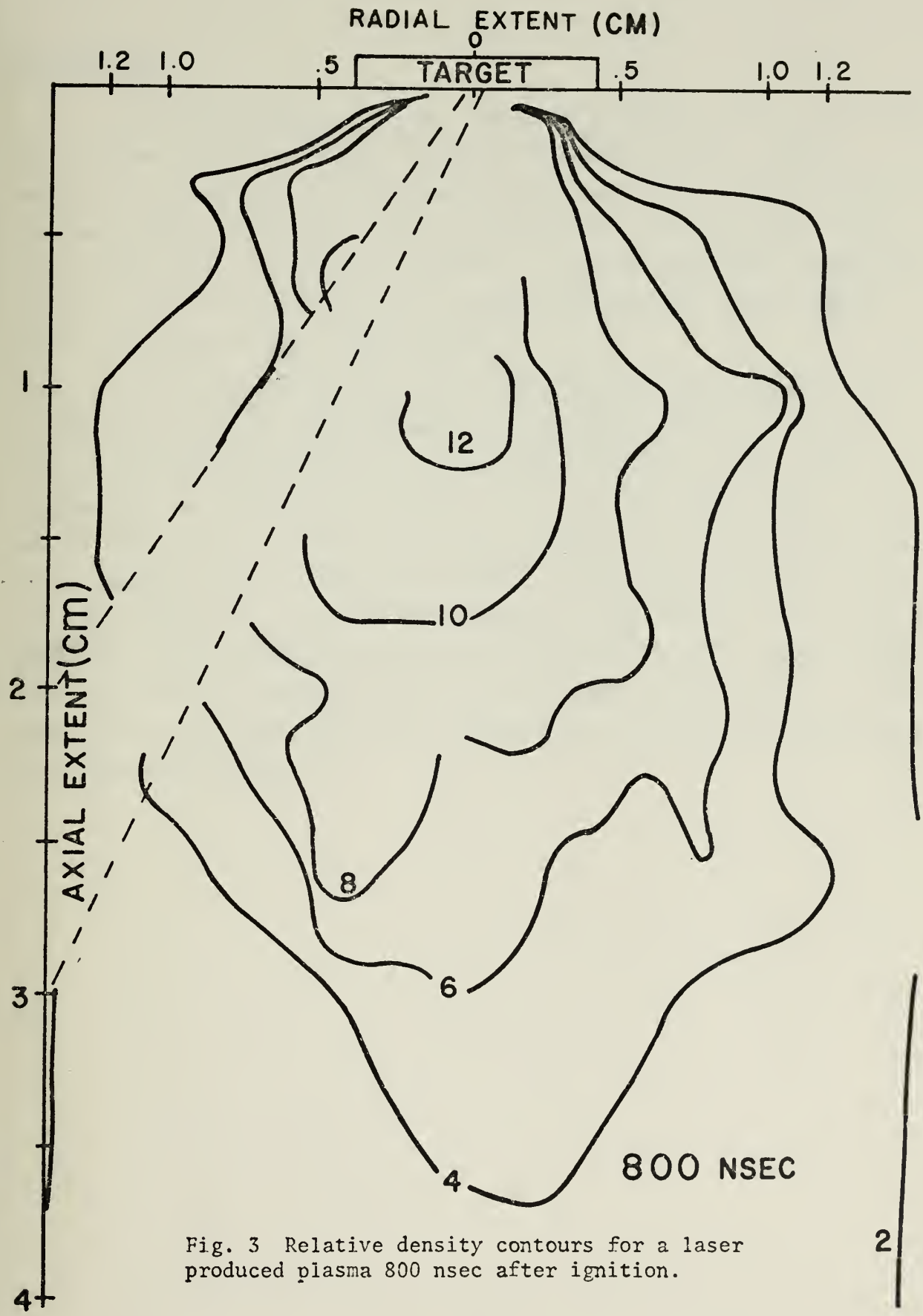

Fig. 3 Relative density contours for a laser produced plasma 800 nsec after ignition.

(U) Electron microscope examination of the focal area on the target produces evidence for shock wave damage of the target. "Large" masses of Al have been spalled from the target. There is also evidence for "splashing" of liquid Al from the target onto the probes when they are located close to the target surface. At these very high irradiances and with these very short pulses, Steverding's model[17] seems to apply during some part of the ignition event.

(U) These investigations also have a bearing upon the nature of the electron emission mechanism which causes prompt ignition. The electron energies corresponding to the emission speeds of the plasma components, see Table IV, are first early = 3.4 eV, second early = 1 eV, main = 3×10^{-2} eV. These results are consistent with an interpretation which suggests that the first two components are caused by a high field emission mechanism, while the main component is thermionic. This interpretation has been discussed by Thomas, Musal and Chou[28]. The structure of the components suggests that the electrons are emitted first and that ions from the target surface are then pulled along behind the electrons by electrostatic forces.

3.0 QUALITATIVE SUMMARY OF TRANSITION PROCESSES

(U) The ignition process is complete as soon as conditions have been established in the air in front of the target surface which will ultimately lead to the production of an LSA wave. A certain number of charged particles must be present (both electrons and ions) and the number of both must increase with time. The transition to full LSA behavior is extremely complex because a large number of processes, both productive and dissipative, are occurring simultaneously. If an LSA wave is to result, the productive mechanisms must dominate. Any mechanism which increases the absolute number or density of electrons is productive, any which decreases the electron population is dissipative. Attention can be focused on the electrons because an electron produced is also an ion produced. The converse of this statement is not necessarily true because electrons can diffuse out of the ionized region when it is small. In most cases this surface leakage is not a dominant consideration, but it is a significant contributor when the dimensions of the ionized volume approach the mean free path of electrons in air. This number depends upon many considerations, but is of the order of 0.5 μm in STP air. In general focal spots, and hence ignition plasmas are much larger; so electron diffusion is a secondary consideration.

(U) The atomic-scale production and dissipation processes are summarized in Figure 4. In the following material A will stand for an unexcited atom or molecule, $\underline{A}^*$ for an atom in an excited state and $\underline{A}^+$ for the singly charged ion of that atom. Multiple ions, A^{2+} etc., and the transition from the molecular to the atomic state will be ignored in this discussion. Both complicate the already complex discussion without significantly contributing to the analysis. The atom-molecule transition is an additional loss mechanism which reduces the effectiveness of the production mechanisms discussed below.

(U) All of the productive processes feed directly or indirectly upon the energy which the laser pulse supplies to the ionized region. This region will be referred to as the plasma, even though in the strictest

$$\underline{\bar{X}} + (\quad) = \underline{\bar{X}}'$$

WHERE $\underline{\bar{X}}$ = A, A^* OR A^+

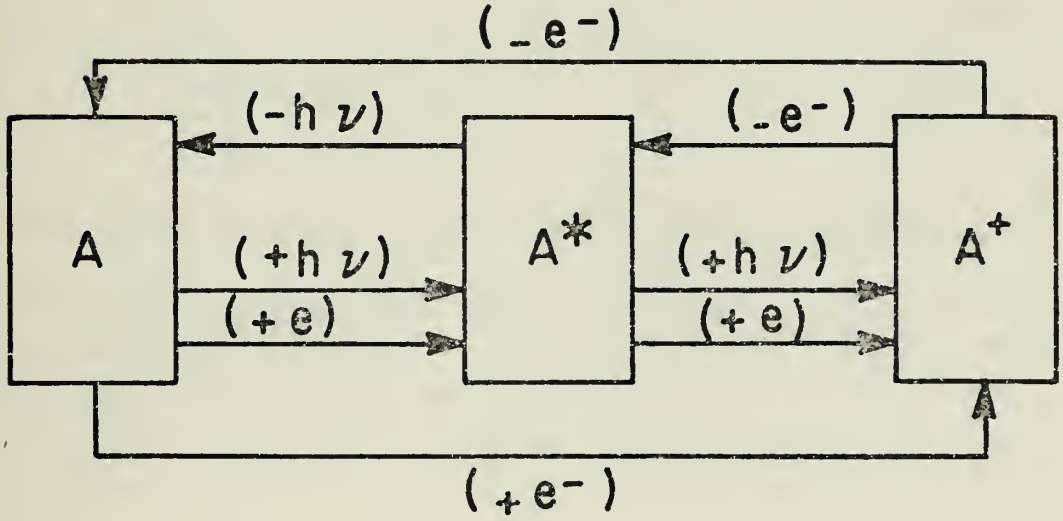

Fig. 4 Schematic representation of production and dissipation processes. Arrows to the right represent an increase in ionization. Arrows to the left represent a decrease in ionization.

sense absolute charge neutrality can not be guaranteed because of electron diffusion and target surface effects.

(U) Because photons couple poorly to atomic mass particles (the mass mismatch is too large) photon-electron processes play the primary role. These processes can be catagorized as bound-bound, bound-free, and free-free where the descriptive words apply to the condition of the electron before, and then after the photon-electron collision. Although these processes must occur 'near' an atom or ion to conserve momentum, the photon-electron collision mechanism dominates the event. The processes are

$$1)\ h\nu + A \rightarrow A^* \qquad \text{(bound-bound)}$$

$$2)\ h\nu + A(A^*) \rightarrow A^+ + e^- \qquad \text{(bound-free)}$$

$$3)\ h\nu + e^- \rightarrow e^{-'} \qquad \text{(free-free)}$$

Mechanisms 1) and 2) combine to produce multiphoton ionization, or on a macroscopic scale, microwave heating of the plasma[28]. The two methods of analysis are formally equivalent. This is a plausible plasma heating mechanism where the laser photon energy exceeds 1.0 eV (Ruby, Nd-Glass, Nd-YAG) but it is not practical for the CO_2 laser photon, which is approximately 0.1 eV.

(U) In the absence of multiphoton ionization, mechanism 3) must be the dominant coupling between the laser pulse and the plasma.

(U) Given a supply of energetic electron from mechanism 3), additional ionization can be produced by electron-atom mechanisms. The productive mechanism is:

$$4)\ e^- + A(A^*) \rightarrow A^+ + 2e^-. \qquad \text{(ionization)}$$

Note that ionization will be facilitated by

$$5)\ e^- + A \rightarrow A^* + e^{-'}. \qquad \text{(excitation)}$$

Mechanism 4) is the ultimate plasma source, while in one sense mechanism 5) is a loss mechanism because it withdraws energy from the electron heating process. It's exact catagorization will depend upon the details

of a particular plasma condition and upon the electron and ion temperatures in that plasma.

(U) Two additional mechanisms:

$$6)\ \bar{e} + A^* \rightarrow A + e^{-'} \qquad \text{(collision de-excitation)}$$

and

$$7)\ \bar{e} + A^+ \rightarrow A + h\nu' \qquad \text{(recombination)}$$

are clearly dissipative.

(U) A great deal of study has been done on photon-electron and electron-heavy particle scattering. Much of the effort required to translate these investigations into forms useful for the LSA transition analysis has been done by Ready[7] (see in particular the sections on spark ignition in air) and by Zel'dovich and Raizer[29] (particularly in Vol. I, which contains the fundamental physical material).

(U) It should be noted that a description of the transition from the atomic interaction mechanisms to plasma ignition is dependent upon some form of transport theory, which in turn requires local (psuedo) thermodynamic equilibrium. The electron equilibration time is such that a well defined electron temperature seems plausible, but the concept of an ion temperature should be used with great caution, because much of the ions' energy may be associated with the streaming of the plasma away from the target. Also, the ion equilibration time is approximately four orders of magnitude greater than the electron equilibration time, which places it uncomfortably close to the entire initiation time of the LSA wave. In summary, the electrons probably have a temperature, the ions may have a temperature, but the electrons and ions are clearly not in thermal equilibirum.

(U) To a good approximation the plasma density will grow exponentially with the number of high energy electron "generations" n, required to reach a given level of ionization. Thus

$$N = N_o \exp\left(\frac{nT_o}{T_c}\right)$$

where T_c is the lifetime of one electron heating cycle:

$$h\nu + e^- \rightarrow e^{-'} ,$$

followed by

$$e^- + A(A^*) \rightarrow A^+ + \bar{e}' .$$

For an ignition plasma of the type studied by Brooks[22] approximately 16 generations are required to produce plasma densities approaching 100% ionization. If N_o were 10 electrons, 43 generations would be required. 99% of the ionization occurs in the last 7 generations. The breakdown process can proceed in times as short as a few nseconds[29].

4.0 PROPAGATION OF LSA WAVES

(U) The preceding two sections discuss the ignition of a plasma at the target surface and the transition of that plasma to a high density state. This section is devoted to the behavior of the system once the plasma has become dense.

(U) The transition process is complete once the plasma reaches a constant density. If this density is less than that established by setting the plasma frequency equal to the laser frequency

$$\frac{N_e e^2}{m} \equiv \nu_\rho = \nu_{laser}$$

$$\nu_\rho = 8.97 \times 10^3 \, N^{1/2} \ (cm^{-3})$$

or

$$N_p(cm^{-3}) = 1.12 \times 10^9/\lambda_p^2 \ (m)$$

the plasma is transparent to the radiation, and the target surface continues to supply material to the plasma. Once the plasma density exceeds the threshold value the plasma becomes opaque and shields the target from the laser pulse.

(U) Three types of behavior have been identified experimentally. When the irradiance, G, is of the order of 10^4 W/cm^2 a plasma is formed at the target surface, but its density never exceeds the plasma frequency threshold. The plasma is in a steady state under the combined influences of the laser irradiation, convection, reradiation and target surface erosion. The resultant PLASMATRON is transparent to the laser radiation; so it remains attached to the target surface. When the irradiance is of the order of 10^5 W/cm^2 the plasma detaches from the target surface and propagates rather slowly ($v \simeq 10^3$ cm/s) back up the laser pulse. The plasma is opaque and protects the target surface from the laser beam. The ignition mechanism

in the air in front of the plasma is very complex. This low velocity disturbance is the LSC wave. Lastly, when the irradiance is of the order of 10^7 W/cm^2, the plasma propagates with a velocity which exceeds the speed of sound and an LSD wave results. The names of the waves come from their similarity to high temperature hydrodynamic waves. The same mathematical models apply; so hydrodynamic theory can be used to describe LSC and LSD waves. This analysis was first developed in the Soviet Union by Raizer[3] and in the West by Ramsden and Savic[30].

(U) Detonation waves are easier to discuss theoretically because a number of simplifying assumptions can be made in the analysis. Combustion waves are more complex and the details of their propagation are less well understood. The analysis here passes from a simple one-dimensional discussion of the relevent hydrodynamic equations to a presentation of the salient characteristics of the LSD wave, and then considers the LSC wave where closed form analytic expressions are less useful.

4.1 HYDRODYNAMIC EQUATIONS

(U) Consider a one-dimensional system of the form shown in Figure 5, which is characteristic of the LSD wave. Here the absorption region is optically thick; so the laser radiation is absorbed there. The wave propagates to the right with speed D. The region denoted "ambient air", will be Region 1 in what follows, and is "ahead of" the wave. The region denoted "relaxation region" will be Region 2, and is "behind" the wave.

(U) The analysis presented here is not sophisticated, but it includes all of the physical processes and variables which are pertinent to this discussion. It differs from the similar hydrodynamic derivations because an energy source term has been included, but the momentum contribution from the laser pulse have been neglected. A more detailed discussion is available in Zel'dovich and Raizer[31]. In the material which follows the thickness of the discontinuity (ℓ in Figure 5) will be neglected.

(U) The variables required to characterize the system are:

p the pressure

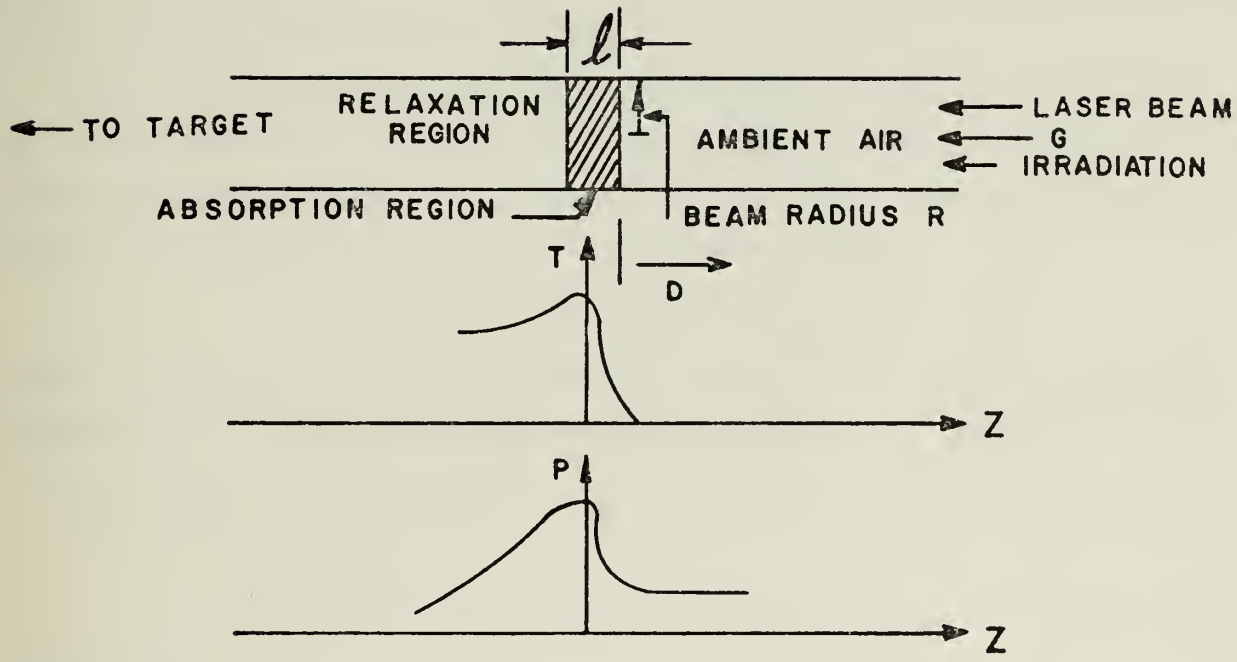

Fig. 5 Temperature and pressure profiles typical of a laser-supported-detonation wave.

ρ	the density or its reciprocal
$V \equiv 1/\rho$	the specific volume
e	the specific internal energy
u	the fluid flow velocity in the LAB system

Occasionally, $h \equiv e + PV$ the specific enthalpy will be used to simplify equations. Here, the term "specific" means "per unit mass". The general term "fluid" has been used rather than "air" or "gas" because the material behind the discontinuity is a plasma.

(U) The analysis considers the conservation of an element of mass, Δm, its momentum, and its energy, as the energy, as the element moves across the discontinuity. In terms of the variables, define a volume element, $\delta\tau$, on each side of the discontinuity. Then,

$$\delta\tau = (\vec{D} - \vec{u}_1) \cdot A\delta t = (\vec{D} - \vec{u}_2) \cdot A\delta t;$$

where the area of the element A, remains constant as it passes through the discontinuity, and of course the same time duration, δt, applies.

(U) Then

$$\Delta m \equiv \rho\delta\tau$$

$$\Delta m = \rho_1(\vec{D} - \vec{u}_1) \cdot A\delta t = \rho_2(\vec{D} - \vec{u}_2) \cdot A\delta t;$$

which gives

$$\rho_1(\vec{D} - \vec{u}_1) = \rho_2(\vec{D} - \vec{u}_2).$$

This conservation of mass relation is most conveniently written as

$$\vec{D}(\rho_2 - \rho_1) = \rho_2\vec{u}_2 - \rho_1\vec{u}_1. \qquad I'$$

(U) Conservation of linear momentum requires that the momentum change of the mass element be equal to the impulse received. Then

$$(P_2 - P_1)\vec{A}\delta t = \Delta m\vec{u}_2 - \Delta m\vec{u}_1.$$

When $\vec{D}$, $\vec{A}$, $\vec{u}_1$, and $\vec{u}_2$ are all parallel this equation simplifies to

$$D(\rho_2 u_2 - \rho_1 u_1) = (P_2 + \rho_2 u_2^2) - (P_1 + \rho_1 u_1^2). \qquad II'$$

This is the simplification which reduces the relation to a one-dimensional form.

(U) Conservation of energy follows from the First Law of thermodynamics:

$$\Delta U = \Delta Q + \Delta W.$$

The element of mass, and hence the quantity, U, contains energy in two forms: the specific internal energy, e, and the specific kinetic energy $(1/2)u^2$. (Watch the units!). Then one writes

$$\Delta U = \Delta m(\varepsilon_2 - \varepsilon_1)$$

where

$$\varepsilon \equiv e + (1/2)u^2.$$

The heat added is the integrated laser flux through A in time δt,

$$\Delta Q = G_o A \delta t$$

and the work done on the element of mass is

$$\Delta W = (P_2 u_2 - P_1 u_1) \cdot A\delta t.$$

When all terms are combined the relation reduces to

$$D(\rho_2\varepsilon_2 - \rho_1\varepsilon_1) = G + (\rho_2 u_2 \varepsilon_2 + P_2 u_2) - (\rho_1 u_1 \varepsilon_1 + P_1 u_1). \qquad \text{III}'$$

(U) These equations can be considerably simplified by transforming to a coordinate system which moves with the discontinuity:

$$u^* = u - D.$$

Note that $\varepsilon \neq \varepsilon^*$ because of the kinetic energy term. The three conservation equations reduce to:

$$\rho_1 u_1^* = \rho_2 u_2^* \equiv j, \qquad \text{I}$$

$$P_1 + \rho_1 u_1^{*2} = P_2 + \rho_2 u_2^{*2}, \qquad \text{II}$$

and

$$(\varepsilon_2 + P_2V_2 + \frac{(1/2)u_2^{*2}}{2}) - (\varepsilon_1 + P_1V_1 + \frac{(1/2)u_1^{*2}}{2}) + \frac{G_o}{\rho_2 u_2^*} = 0. \qquad \text{III}$$

It is convenient to define

$$q \equiv G_o/\rho_2 u_2^*$$

where q is the specific energy which the element of mass has acquired from the laser pulse as it moves through the absorption region, see Figure 5.

(U) So far only three relations have been specified relating four unknowns, but a number of useful results can be obtained before the equation of state of a specific material is introduced. The equations are most easily manipulated when written in terms of V. With this modification, Eq. I becomes

$$u_1^*/u_2^* = V_1/V_2,$$

and Eq.s I and II can be manipulated to obtain

$$j \equiv u_2^*/V_2 = \sqrt{\frac{P_2-P_1}{V_1-V_2}} = u_1^*/V_1 \qquad (1)$$

These relations are of special use when $u_1 = 0$ (ambient air at rest); so that $u_1^* = -D$. With this additional condition

$$|D| = V_1\sqrt{\frac{P_2-P_1}{V_1-V_2}}, \qquad (2)$$

this is the speed of the discontinuity in the LAB coordinate system.

(U) It is possible to show that $u_1 \leq D$ if the discontinuity is to propagate as indicated, so u_1^* must always be negative. But V_1 must be positive; so

$$j \equiv \sqrt{(P_2-P_1)/(V_1-V_2)}$$

must be intrinsically negative. This factor will <u>always</u> be assumed to be negative.

(U) When $u_1 = 0$, Eq. I can be written (use Eq. 2)

$$u_2 = \sqrt{(P_2-P_1)/(V_1-V_2)} \tag{3}$$

N.B. that u_2 is in the LAB system. $u_2 < D$ for all possible discontinuities (otherwise the material behind the discontinuity would catch up to it!), so u_2^* must also be negative.

(U) It is convenient to remove the microscopic variables u_1^{*2} and u_2^{*2} from Eq. III. From Eq. I

$$u_2^{*2} - u_1^{*2} = -(V_1+V_2)(P_2-P_1), \tag{4}$$

and Eq. III becomes

$$\varepsilon_2-\varepsilon_1 + 1/2(V_2-V_1)(P_1+P_2) = q \tag{5}$$

The negative sign in the definition of q was chosen so that Eq. 5 could be interpreted physically. It is consistent with the fact the u_2^* is intrinsically negative; so q as defined will always be positive.

(U) To proceed further one must assume an equation of state for the material. The ideal gas will be used in this discussion because it is sufficient for demonstrative purposes, even though it can hardly be expected to describe a plasma correctly. In terms of the specific heat ratio (C_p is the specific heat at constant pressure, C_v at constant volume)

$$\gamma \equiv C_p/C_v , \tag{6}$$

the ideal gas law can be written as

$$P = (\gamma-1)\rho e. \tag{7}$$

At times it is more convenient to define a temperature

$$T \equiv e/C_v \tag{8}$$

(note that C_v is assumed to remain constant); then

$$P = (\gamma-1)\rho C_v T. \tag{9}$$

A useful auxiliary relation is

$$\left(\frac{\gamma}{\gamma-1}\right)PV = e + PV = h = C_p T \tag{10}$$

(U) These basic relations will now be applied to various LSA wave propagation conditions.

4.2 ONE-DIMENSIONAL LSD WAVES

(U) Detonation waves occur when the speed of the wave exceeds the speed of sound in the ambient air, $D > c_1$. The wave propagation is not stable unless it also meets the condition $u_2 \leq c_2 \leq D$, where c_2 is the speed of sound behind the discontinuity. With these conditions the discontinuity propagates as a shock wave, and many of the analytic results obtained from shock wave studies also apply to LSD wave propagation.

(U) The system is easiest to analyze if the CHAPMAN-JOUGET condition is applied:

$$u_2^* = c_2,$$

which,when combined with the ideal gas medium, gives

$$u_2^{*2} = c_2^{\,2} = \gamma_2 P_2 V_2. \tag{11}$$

Zel'dovich and Raizer[31] discuss the meaning of this condition in considerable detail.

(U) When Eq. 11 is used with Eq. II, one obtains

$$P_2 = \frac{P_1V_1 + u_1^{*2}}{V_1(\gamma_2 + 1)} \quad ; \tag{12}$$

in conjunction with Eq. I, it gives

$$V_2 = \left(\frac{u_1^{*2} + P_1V_1}{V_1} \right)\left(\frac{\gamma_2}{\gamma_2 + 1} \right) \quad , \tag{13}$$

and in Eq. III with Eq. 10 it reduces to

$$\left(\frac{\gamma_2}{\gamma_2 - 1} \right)P_2V_2 - \left(\frac{\gamma_1}{\gamma_1 - 1} \right)P_1V_1 - \frac{1}{2}\gamma_2P_2V_2 - \frac{u_1^{*2}}{2} = q. \tag{14}$$

Note that the change in medium properties behind the shock front has been accounted for in this analysis by allowing $\gamma_1 \neq \gamma_2$. If one now eliminates P_2 and V_2 from Eq. 14, the resultant equation is a bi-quadratic in u_1^{*2}. The solution to this equation, with the replacement

$$P_1V_1 + (\gamma_1 - 1)C_{v_1}T_1$$

is

$$u_1^* = \left\{ \sqrt{1/2(\gamma_2-1)[(\gamma_2+1)q + (\gamma_1+\gamma_2)C_{v_1}T_1]} \right\}^{1/2}$$

$$+ \left\{ \sqrt{1/2(\gamma_2+1)[(\gamma_2-1)q + (\gamma_2-\gamma_1)C_{v_1}T_1]} \right\}^{1/2} . \tag{15}$$

This equation becomes very simple in the strongly illuminated condition where $q >> C_{v_1}T_1$ (the specifid internal energy of the ambient gas is negligible compared to the specific energy added by the laser). It becomes,

$$|u_1^*| = |D| = \left\{ 2(\gamma_2^2 - 1)q \right\}^{1/2} . \tag{16}$$

Now restate Eq. 12 to provide the pressure ratio,

$$\frac{P_2}{P_1} = \frac{u_1^{*2} + (\gamma_1 - 1)C_{V_1}T_1}{(\gamma_2+\gamma_1)(\gamma_1 - 1)C_{V_1}T_1}, \tag{17}$$

and Eq.s 13 and 17 provide the volume ratio

$$\frac{V_2}{V_1} = \frac{\gamma_2}{\gamma_2+1}\left[\frac{u_1^{*2} + (\gamma_1 - 1)C_{V_1}T_1}{u_1^{*2}}\right]. \tag{18}$$

If one now uses the requirement $(\gamma_1 - 1)C_{V_1}T_1 << u_1^{*2}$, Eq. 10 reduces to

$$\frac{V_2}{V_1} = \frac{\gamma_2}{\gamma_2+1} \tag{19}$$

which applies in the strong shock limit of a strongly fed wave which also satisifies the CHAPMAN-JOUGET condition. To the same approximation

$$\frac{P_2}{P_1} = \frac{2(\gamma_2-1)}{(\gamma_1-1)}\frac{q}{C_{V_1}T_1} = \frac{\gamma_1 D^2}{(\gamma_2+1)C_1^2}$$

$$\frac{P_2}{P_1} \doteq \frac{\gamma_1}{\gamma_2+1}M^2 \tag{20}$$

where M is the Mach Number of the detonation wave motion.

(U) If one replaces q by its definition in Eq. 16, one obtains a relation between the wave speed D and the irradiance of the laser:

$$D = [2(\gamma_1^2 - 1)V_1 G_o]^{1/3} \tag{21}$$

Note that this result depends upon the ambient density in front of the shock, the specific heat ratio behind the shock, and the irradiance. The relation between D and G has been well tested experimentally.

4.3 ONE-DIMENSIONAL LSC WAVE

(U) Combustion waves occur when the velocity of propagation of the disturbance is less than the velocity of sound. Velocities for LSC phenomena range from D = 0, the plasmatron, to the order of a few meters/second. Here the D = 0 case is specifically excluded.

(U) The LSC disturbance is a more complex structure than is the LSD wave as sketched in Figure 6. This figure, from the work of Jackson and Neilsen[32], is the result of a computer computation. Its qualitative features agree very well with the experimental data available on LSC and LSD waves.

(U) The LSC wave structure is conveniently divided into three regions: A, the ambient air in front of the disturbance; B, the transition region, which has been warmed and which contains some ionized particles, but which is transparent to the laser photons; and C, the plasma, which is opaque to the laser photons. The electron density and temperature increase continuously with distance from the wave front so that at the plasma front the plasma frequency of the ionized medium equals the frequency of the incident laser light.

(U) The LSC wave differs from the LSD wave because the disturbance created by the wave front is not sufficiently intense to produce the electron density required to support the plasma; so additional ionization must be generated by the plasma. For the LSD wave the two fronts coalesce and the analysis is much simpler.

(U) Because of the more complex structure, the simple conservation law analysis of the LSD system contained in Eq.s I, II, and III is no longer appropriate. It could be applied between regions A and C, but most of the interesting phenomena which control the wave development occur in region B. In region B the parameters are functions of distance

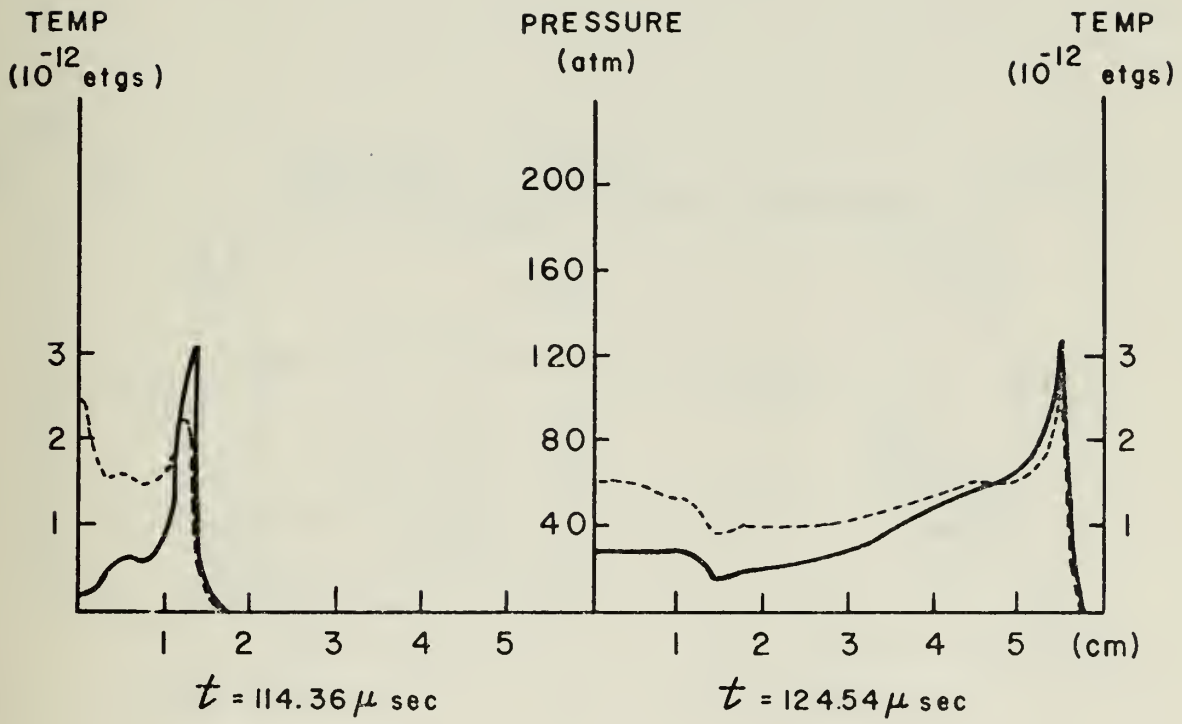

Fig. 6A One-dimensional LSD wave driven by a CO_2 laser flux of 1 x 10^7 watts/cm^2 decoupling of high temperature region and shock wave does not occur V_{LSD} = 4.0 x 10^5 cm/sec.

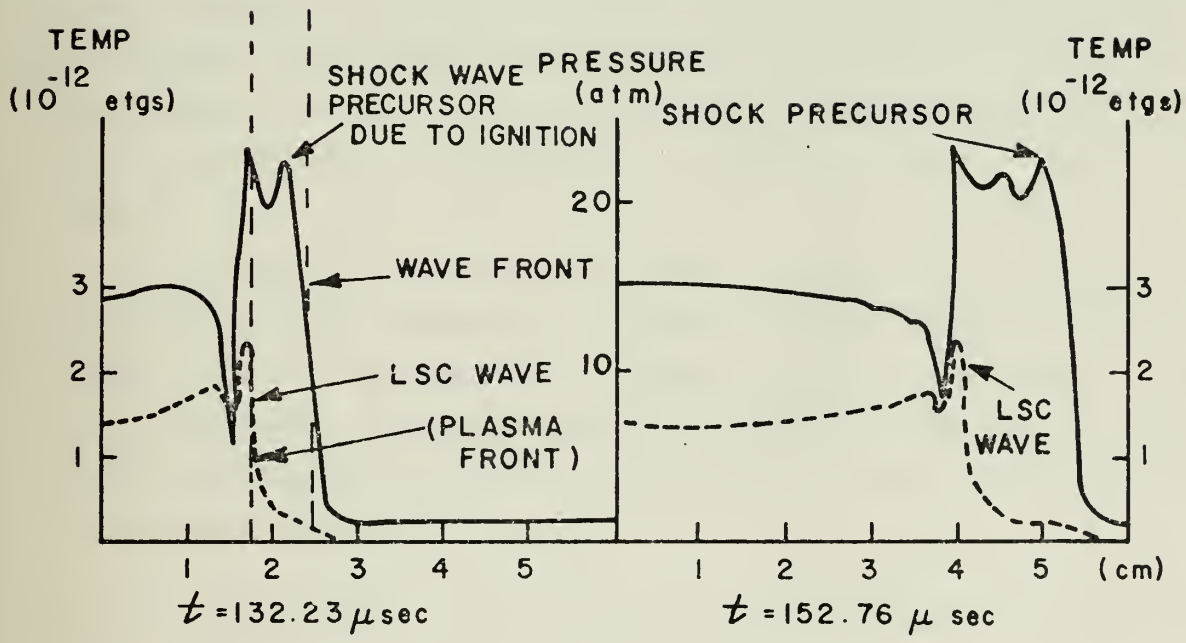

Fig. 6B One-dimensional LSC wave and shock wave precursor driven by a CO_2 laser flux of 1×10^6 watts/cm^2.

$V_{LSC} = 1.1 \times 10^5$ cm/sec and $V_{SHOCK} = 1.4 \times 10^5$ cm/sec

from the wave front; so a full divergence theory analysis is required. In addition, the functional variations are driven by the atomic level process discussed in Section 2; so the resultant non-linear differential equations are extremely complicated.

(U) Here it seems appropriate to discuss the model and the phenomenological parameters, but a presentation of the actual numerical methods used to solve the equations would go beyond the intent of this survey. The interested reader will be referred to the current literature at the appropriate points in the discussion. In many respects this presentation draws heavily upon Nielsen and Canavan[5], but there are significant variations from their notation. The original analysis of LSC waves performed by Raizer[33], has strongly influenced all subsequent studies.

(U) Because the LSC wave propagates so slowly, to a very good approximation the pressure may be assumed constant throughout the disturbance and the conservation of momentum condition contributes nothing to the analysis. Similarly, there is very little mass flow; so effectively only the energy conservation condition remains. This condition, written in differential form is

$$\mathrm{Div}(\rho v h + P v) = Q.$$

Here h is the enthalpy and Q contains all of the energy source and sink terms. Three terms can be identified in Q:

$$Q = \Phi + \Psi + \xi \tag{22}$$

where Φ is the radiation term, Ψ the heat conduction term, and ξ is the electron transport term. Each of these terms operates somewhat differently in the three regions. Q vanishes in region A, because by definition the medium is undisturbed there. The laser supplies energy in region C, because the plasma is opaque, so Φ is a source term which can be written

$$\Phi = K_o G_o(x) \tag{23}$$

where K_o is the absorption coefficient, and G(x) is the residual laser flux at distance x from the wave front which is taken as the origin. The laser intensity in turn must satisfy

$$\frac{dG}{dx} = -KG \tag{24}$$

subject to the boundary condition $G(o) = G_o$, the laser irradiance.

(U) The absorption coefficient, K, is a strongly varying function of temperature, see Figure 7. Because the coefficient rises so sharply, in most calculations it is approximated by the function

$$\begin{aligned} K(T) &= 0.0 \qquad T < 12{,}000°K \\ &= 0.7\ cm^{-1} \qquad T > 12{,}000°K \end{aligned} \tag{25}$$

Other investigations prefer to set $K(T) = 0.6\ cm^{-1}$ when $T > 1.0$ eV[32].

(U) In region C, the thermal conduction term, Ψ, is a loss term. It supplies much of the energy which increases the temperature of region B. The thermal conductivity of air, β, is an extremely complicated function of temperature, see Figure 8. A convenient approximation for β is[18]

$$\beta = 2 \times 10^{-6}\ T\ (\text{watts/cm °K}). \tag{26}$$

The heat flux is given by

$$\Psi = -\beta \frac{d^2T}{dx^2}\ . \tag{27}$$

To a reasonable approximation the temperature of the plasma is constant, $T_p \simeq 1$ eV; so there is heat conduction from the plasma into region B. By analogy, with chemical combustion waves, Raizer[33] felt that heat conduction would supply sufficient energy to increase the temperature of region B to "combustion". Careful calculation by Hall, et.al.[18] and Thomas, et.al.[28] have shown that this is not the case.

(U) Jackson and Nielsen[32] have investigated the heating of region B by radiation transport from the plasma of region C. The opaque 1 eV temperature plasma emits strongly throughout the visible region of the spectrum and also well into the ultraviolet. The dominant radiation heating contribution in region B comes from this source rather than from the laser beam. Effectively, the plasma serves as a frequency converter for the laser energy, and re-emits it in a spectral region

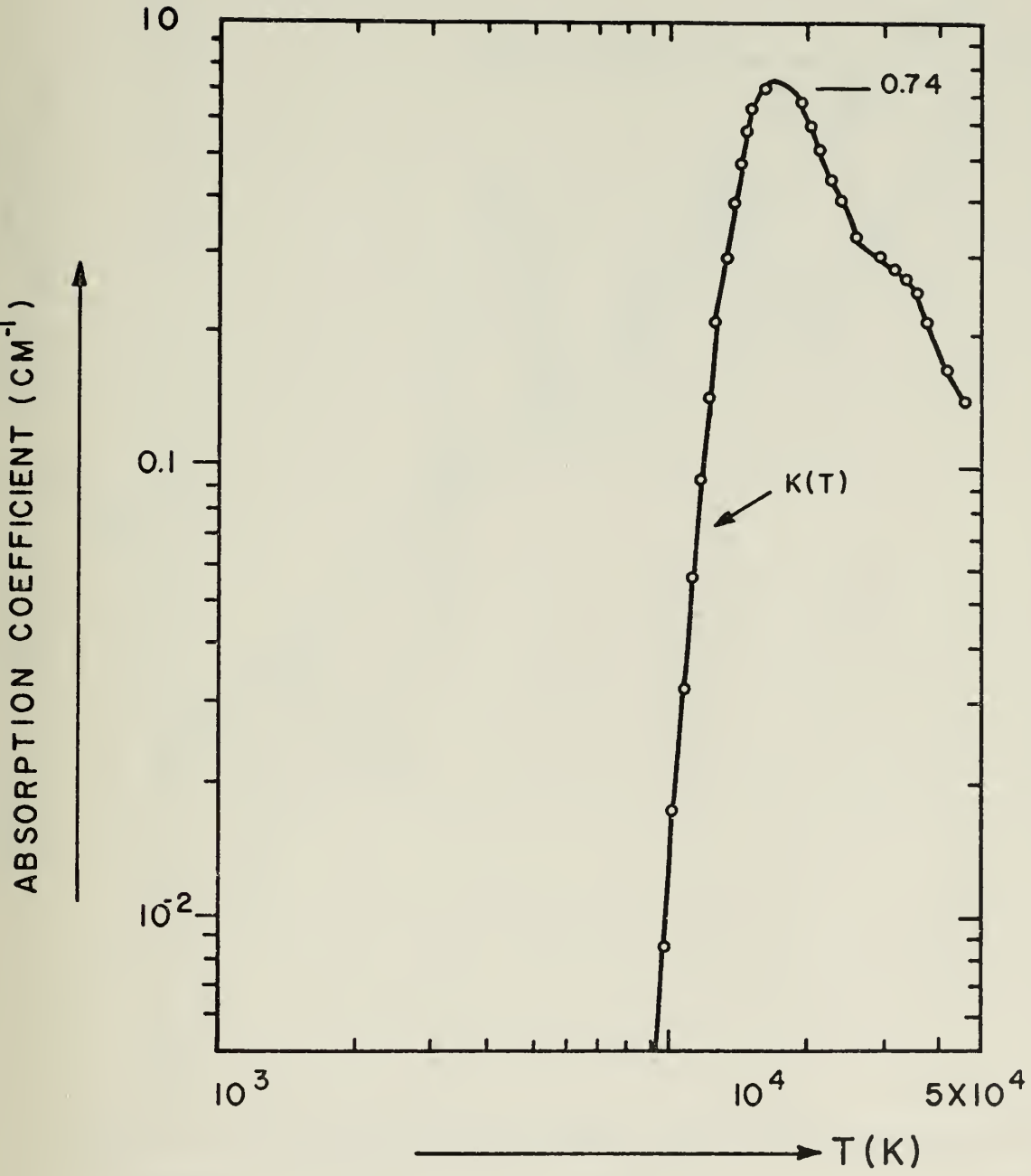

Fig. 7 Abortion coefficient of a carbon dioxide laser in air as a function of temperature. From reference 18.

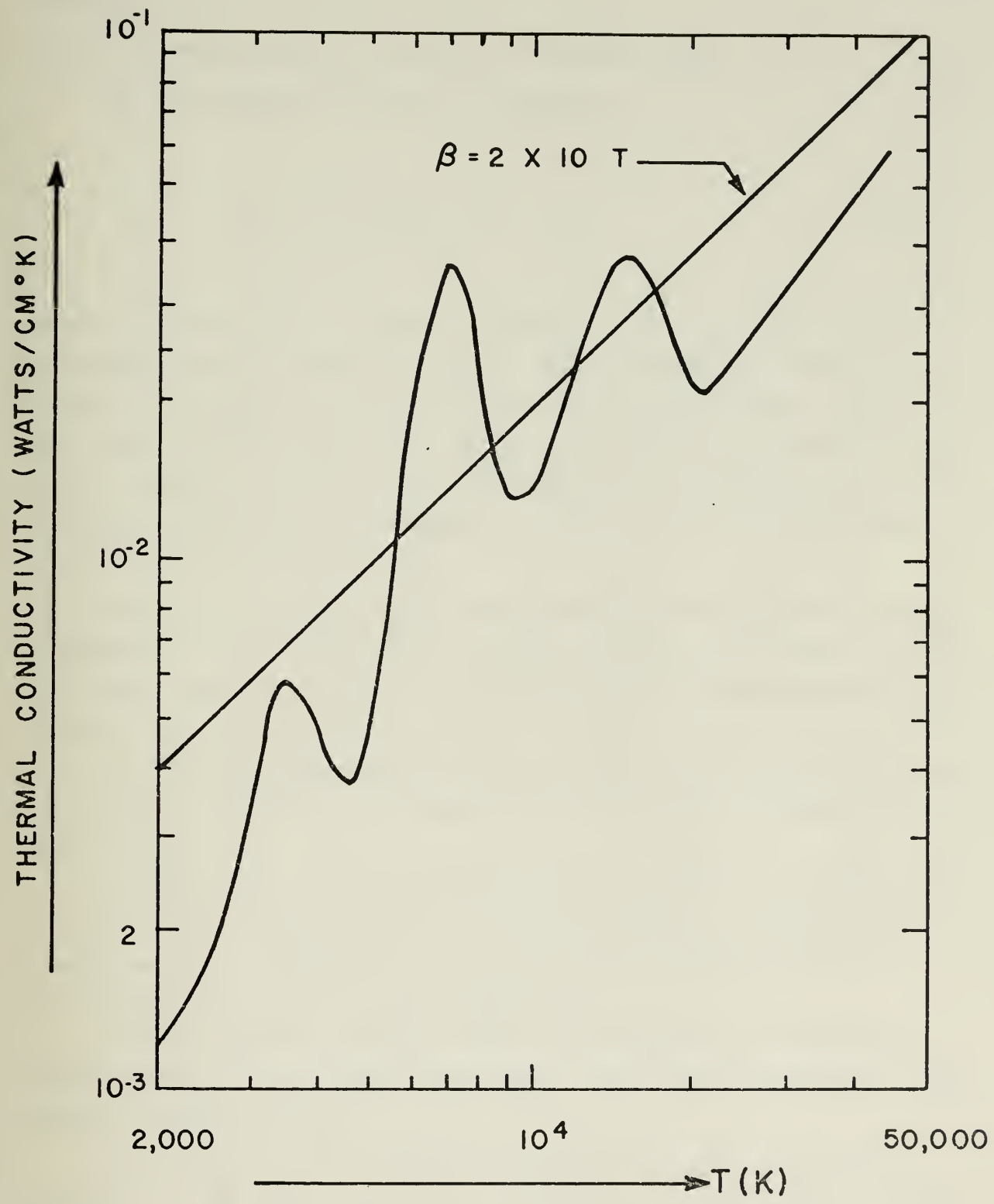

Fig. 8 Thermal conductivity of air as a function of temperature. From reference 18.

where the weaker plasma of region B is already opaque.

(U) The radiant flux term is written as

$$\Phi = -c \int_{\infty}^{\infty} d\nu K'_{\nu}(G_{\nu\rho}(T) - G_{\nu}) \qquad (28)$$

in the Jackson and Nielsen model. Here G_{ν} is the irradiance per unit frequency from all sources and $G_{\nu\rho}(T)$ is the equilibrium radiative energy flux density. In this formulation Φ is a loss term in region C and a source term in region B. The simple attenuation approach of Eq. 23 comprises one part of this expression. The coefficient K'_{ν} is the absorption coefficient at frequency ν corrected for induced emission, see Zel'dovich and Raizer[31].

(U) This coupling of the various portions of the LSC wave through radiation transport makes the entire model strongly non-linear. Still, the model equations can be solved analytically if three assumptions are made:

1) The absorption coefficient must be treated as a step function as in Eq. 25. (Jackson and Nielsen use 0.6 cm^{-1} with a threshold temperature of 1 eV).

2) The ratio $\beta(T)/C_p(T)$ is set equal to a constant $f = 1.0 \times 10^{-3}$ gm/cm-sec. The enthalpy of air is shown in Figure 9, together with a useful analytic approximation. The relation $C_p = (\partial h/\partial T_p)$ and this approximation give $f \approx 2 \times 10^{-3}$ gm/cm-sec.

3) The radiative transport term Φ, is written as an exponential heating term in front of the plasma front and a constant absorption term behind the plasma front.

(U) The system of equations can then be solved by a series of iterations which adjust the values of the necessary parameters. Jackson and Nielsen find that the most important contribution energy contributes from radiation transport comes in the range 14.5 eV $\leq \nu \leq$ 20 eV, which is well into the uv region. Account must be taken of the anisotrophy of the radiation field. The authors use 19 frequency groups to establish the

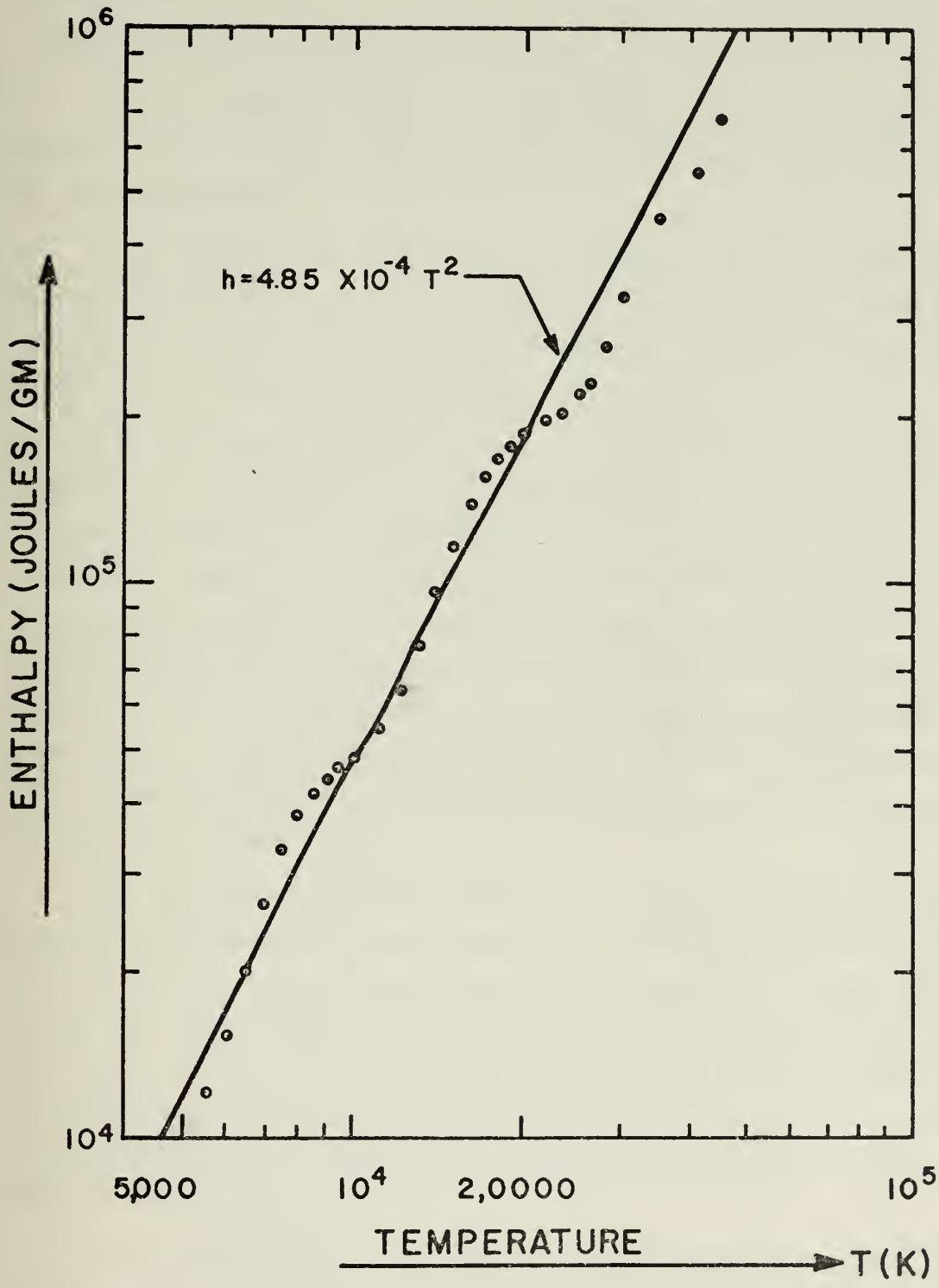

Fig.9. Enthalpy of air as a function of temperature. From reference 18.

self-consistent solutions.

(U) The model preduces the correct trend of the propagation velocity, D, with the laser irradiance, β, but agreement in magnitude is not satisfactory; see Figure 10.

(U) Jackson[34] has shown that the presence of the target surface forces a streaming velocity upon the air in which the LSC wave is propagating; so that the experimentally determined velocity is considerably larger than the radiation transport model predicts.

(U) The final transport term, ξ, the electron fluence, has apparently not been considered by any investigator. Clearly region C contains a high density of electrons and no free electrons are present in region A; so there must be a diffusion of electrons into region B driven by a concentration gradient. The effect is complicated by the fact that ions must accompany the electrons to maintain charge neutrality; so the model is one in which a high density plasma diffuses into a low density plasma. This type of an analysis would require an additional conservation law, the number of particles, and a kinetic theory approach to the spatial distribution of particles.

(U) One other important idea is suggested by Figure 6, which depicts both LSC and LSD waves produced by the same computer code. With the LSC wave irradiation condition, the LSC wave, the plasma front, falls behind the shock front; so the wave presents the characteristic double structure. As the irradiance increases, the speed of the plasma front increases until finally the two front propagate together as an LSD wave. Apparently there is a continuous variation from plasmatron through LSC behavior to LSD behavior.

(U) Jackson[35] has calculated the irradiance at which the LSD behavior should appear. He finds

$$G_t = \left[\frac{(\gamma-1)^{1/2}}{2\gamma} \right] \rho_A h_B^{3/2}$$

where ρ_A is the ambient air density and h_B is the enthalpy in region B.

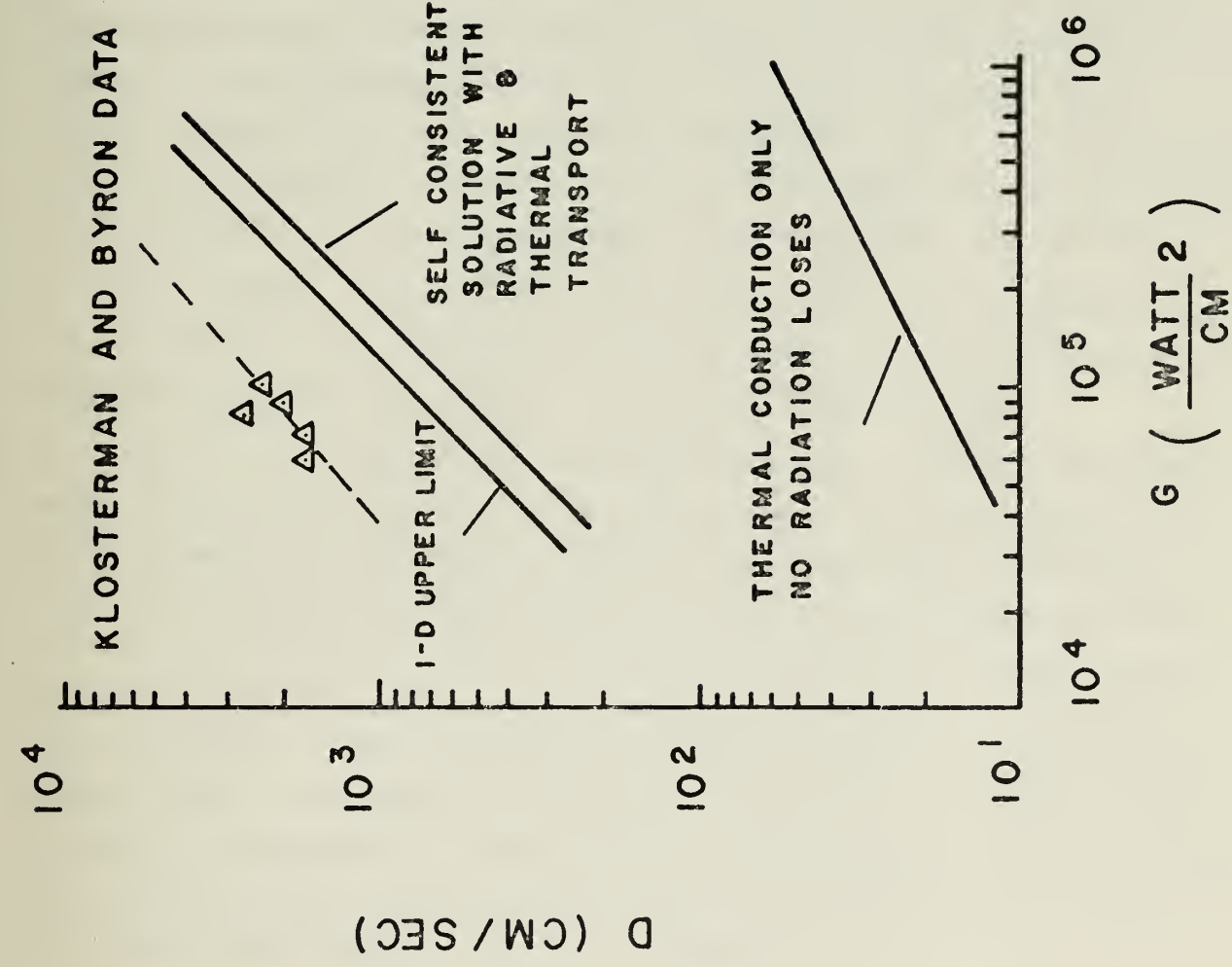

Fig. 10 Plasma wave velocity as a function of irradiance.

With reasonable values for the parameters, $H_t = 2 \times 10^7$ W/cm^2 which agrees quite well with the experimental results of 2.25×10^7 W/cm^2 [18].

4.4 LSA WAVES IN TWO-DIMENSIONS

(U) The geometry of any LSA wave system is clearly cylindrical as soon as it enters the transition phase. The one-dimensional analyses presented here are only approximations which have meaning when radial effects (across the wave) can be neglected relative to longitudinal effects (parallel to the direction of propagation). When ignition, transition, and propagation are under study radial effects introduce additional loss mechanisms which withdraw energy and electrons from the plasma.

(U) Magnetic confinement of the plasma, caused by its motion, will be neglected in this discussion. It is an additional consideration which will tend to reduce the effect of the radial loss mechanisms.

(U) The significance of the radial direction is effectively determined by the diameter of the laser beam in the volume under study. A small diameter beam allows significant radial transport of electrons, heat, and radiation; a large diameter beam does not. Raizer[3] has shown that when the amount of radial of expansion is small the energy balance equation should be corrected by the replacement $G \rightarrow G/(1 + \ell/R)$, where R is the radius of the laser beam, and ℓ is the length of the absorption region; that is the depth of the plasma in region C of the last section. Jackson and Nielsen[32] have done rather careful calculations which confirm that radial losses are of secondary importance in the analysis of LSA waves when the condition $\ell << R$ is satisfied.

5.0 SUMMARY

(U) This article reviews the initiation and propagation of LSC and LSD waves. It concludes that prompt ignition requires that electrons be emitted from the target surface, most probably at physical features and/or inclusions in the surface. The electrons are followed by ions extracted from the surface by electrostatic forces. If the irradiation is sufficiently intense the plasma moves away from the surface and feeds upon the incident laser radiation. The plasma is accompanied by a shock wave. At intermediate irradiance levels the plasma falls behind the shock wave and an LSC wave results. For irradiance levels above $\sim 2 \times 10^7$ W/cm^2 the plasma and shock wave move together as an LSD wave.

REFERENCES

1. 1973 DoD Laser Effects/Hardening Conference, V. I, Norman F. Harmon, Editor, the Mitre Corporation, M73-115, ARPA Order No. 2539.

2. P. E. Nielsen, Laser Effects/Hardening Conference, V. V, p. 15 (1973)

3. Yu. P. Raizer, "Heating of a Gas by a Powerful Light Pulse", Soviet Physics-JETP 21, 1009 (1965)

4. P. E. Nielsen and G. H. Canavan, "Laser Absorption Waves", Air Force Weapons Laboratory Laser Digest, LRD-71-2, p. 110 (1971)

5. P. E. Nielsen and G. H. Canavan, Air Force Weapons Laboratory Laser Digest, LRD-71-2 (Dec 1971) AD-889 417L, p. 123.

6. C. T. Walters, Laser Effects/Hardening Conference, V. V, p. 179 (1973)

7. John F. Ready, "Effects of High Power Laser Radiation", Academic Press, New York (1971)

8. S. I. Anisimov, A. M. Bonch-Bruevich, M. A. El'Yashevich, Ya. A. Imas, N. A. Paulenko, and G. S. Romanov, "Effects of Powerful Light Fluxes on on Metals", Soviet Physics-Technical Physics 11, 945 (1967)

9. S. Dushman, Rev. Mod. Phys. 2, 381 (1930)

10. F. K. Richtmyer, E. H. Kennard, and J. N. Cooper, Introduction to Modern Physics (McGraw-Hill Book Co., N.Y., 1969), 6th Ed., p. 580 et. seq.

11. J. F. Ready, Phys. Rev. 137, A620 (1965)

12. H. M. Musal, Laser Effects/Hardening Conference, V. V, p. 157 (1973)

13. R. H. Fowler and L. W. Nordheim, Proc. Roy. Soc. A119, 173 (1928)

14. C. Caroli, D. Lederer-Rozenblatt, B. Roulet, and D. Saint-James, Phys. Rev. B10, 861 (1974)

15. J. S. Blakemore, Solid State Physics (W. B. Saunders Co., Phila., Pa 1969), p. 176, et. seq.

16. C. Herring and M. H. Nichols, Rev. Mod. Phys. 21, 185 (1949) and W. B. Nottingham, Handbook der Physik, 21, 1. (Springer 1956)

17. B. Steverding, J. Appl. Phys. 45, 3507 (1974)

18. R. B. Hall, W. E. Maher, and R. S. P. Wei, "An Investigation of Laser Supported Detonation Waves", AFWL-TR-73-28

19. M. C. Fowler and D. C. Smith, Laser Effects/Hardening Conference, V. V, p. 41 (1973)

20. R. W. Conrad, D. W. Mangum, and W. H. Gurley, Laser Effects/Hardening Conference, V. V, p. 55 (1973)

21. P. D. Thomas, Laser Effects/Hardening Conference, V. V, p. 69 (1973)

22. K. M. Brooks, Sr., "An Investigation of Early Disturbances Found in Association with Laser Produced Plasmas", M. S. Thesis, Naval Postgraduate School, December 1973 (unpublished)

23. E. L. Klosterman, S. R. Byron , and J. F. Newton, "Laser Supported Combustion Wave Study", Report No. 73-101-3, Mathematical Sciences Northwest, Inc., Feb. 1973

24. Yu. V. Afanasyev, O. V. Krohkin, and G. V. Skizkov, IEEE Journal of Wuantum Electrontics, V. QE-2, 483 (1966)

25. W. L. Knecht, Appl. Phys. Letters 6, 99 (1965)

26. N. G. Basov, V. A. Boiko, B. A. Dement'ev, O. N. Krohkin, and G. V. Skizkov, Soviet Physics-JETP 24, 659 (1967)

27. B. Wegener, "Measurement of Early Magnetic Fields in Laser Produced Plasmas", M. S. Thesis, Naval Postgraduate School, June 1974 (unpublished)

28. P. D. Thomas, H. M. Musal, and Y. S. Chou, Laser Beam Interaction - Part II, Lockheed Missiles and Space Co., LMSC-D403747, August 1974 (unpublished)

29. P. F. Browne, Proc. Phys. Soc. 86, 1323 (1965)

30. S. A. Ramsden and P. Savis, Nature 203, 1217 (1964)

31. Ya. B. Zel'dovich and Yu. P. Raizer, Physics of Shock Waves and High Temperature Thermodynamic Phenomena, Ed: W. D. Hayes and P. F. Probstein, Academic Press (1966)

32. J. P. Jackson and P. E. Nielsen, AFWL/LD, AFWL-TR-74-100, p. 210 May 1974

33. Yu. P. Raizer, Soviet Physics-JETP 31 , 1148 (1970)

34. J. P. Jackson, AFWL/LD, AFWL-TR-74-241, p. 120 (1974)

35. J. P. Jackson, AFWL/LD, AFWL-TR-74-241, p. 176 (1974)

DISTRIBUTION LIST

1.	Defense Documentation Center Cameron Station Alexandria, Virginia 22314	2
2.	Library, Code 0212 Naval Postgraduate School Monterey, California 93940	2
3.	Department Chairman, Code 61 Department of Physics and Chemistry Naval Postgraduate School Monterey, California 93940	2
4.	Professor Don E. Harrison, Jr. Department of Physics and Chemistry Naval Postgraduate School Monterey, California 93940	4
5.	Professor John R. Neighbours Department of Physics and Chemistry Naval Postgraduate School Monterey, California 93940	2